Investigating the response of LAI to droughts in southern African vegetation using observations and model-simulations.

Shakirudeen Lawal[1], Stephen Sitch[2], Danica Lombardozzi[3], Julia E.M.S. Nabel[4], Hao-Wei Wey[4], Pierre Friedlingstein[5], Hanqin Tian[6], Bruce Hewitson[1]

[1]Climate System Analysis Group, Department of Environmental and Geographical Science, University of Cape Town, Cape Town, 7700, South Africa

[2]College of Life and Environmental Sciences, University of Exeter, Exeter EX4 4QE, UK

[3]National Center for Atmospheric Research, Climate and Global Dynamics, Terrestrial Sciences Section, Boulder, CO 80305, USA

[4]Max Planck Institute for Meteorology, Hamburg, Germany

[5]College of Engineering, Mathematics and Physical Sciences, University of Exeter, Exeter EX4 4QF, UK

[6]School of Forestry and Wildlife Sciences, Auburn University, 602 Ducan Drive, Auburn, AL 36849, USA

*Corresponding author: lasd_dr@yahoo.com

Abstract

In many regions of the world, frequent and continual dry spells are exacerbating drought conditions, which have severe impacts on vegetation biomes. Vegetation in southern Africa is among the most affected by drought. Here, we assessed the spatiotemporal characteristics of meteorological drought in southern Africa using the Standardized Precipitation Evapotranspiration Index (SPEI) over a 30-year period (1982 – 2011). The severity and the effects of droughts on vegetation productiveness were examined at different drought time-scales (1- to 24-month time-scales). In this study, we characterized vegetation using the Leaf Area Index, after evaluating its relationship with the Normalized Difference Vegetation Index. Correlating the LAI with the SPEI, we found that the LAI responds strongly (r = 0.6) to drought over the central and southeastern parts of the region, with weaker impacts (r < 0.4) over parts of Madagascar, Angola and western parts of South Africa. Furthermore, the latitudinal distribution of LAI responses to drought indicates a similar temporal pattern but different magnitudes across timescales. The results of the study also showed that the seasonal response across different southern African biomes varies in magnitude and occurs mostly at shorter to intermediate timescales. The semi-desert biome strongly correlates (r = 0.95) to drought as characterized by the SPEI at 6-month timescale in the MAM (summer) season, while the tropical forest biome shows the weakest response (r = 0.35) at 6-month timescale in the DJF (hot and rainy) season. In addition, we found that the spatial pattern of change of LAI and SPEI are mostly similar during extreme dry and wet years, with the highest anomaly observed in the dry year of 1991; and we found different temporal variability in global and regional responses across different biomes.

We also examined how well an ensemble of state-of-the-art dynamic global vegetation models (DGVMs) simulate the LAI and its response to drought. The spatial and seasonal response of the LAI to drought is mostly overestimated in the DGVM multi-model ensemble compared to the response calculated for the observation-based data. The correlation coefficient values for the multi-model ensemble are as high as 0.76 (annual) over South Africa, and 0.98 in MAM season over the temperate grassland biome. Furthermore, the DGVM model ensemble shows positive biases (3-month or longer) in the simulation of spatial distribution of drought timescales and overestimates the seasonal distribution timescales. The results of this study highlight the areas to target for further development of DGVMs and can be used to improve the models' capability in simulating the drought-vegetation relationship.

Keywords: Drought intensity; Drought indices; Standardized precipitation evapotranspiration index; DGVMs; southern Africa; Drylands

1   Introduction

Drought can be described as a natural occurrence whereby the natural accessibility of water for a region is beneath the normal state over a long period of time (Xu *et al.,* 2015). Globally, it is considered one of the world's most important climate risks, with significant environmental, social and ecological impacts on different sectors (e.g. agriculture, forestry, hydrology) and human lives (Naumann *et al*., 2018). Increasing trends in the occurrence and severity of drought in West Africa and Mediterranean have huge impacts on water resources and agriculture (Sultan and Gaetani, 2016). In southern Africa, a region regarded as a climate hotspot because of the projected impacts of climate change on its numerous endemic vegetation, an understanding of these impacts is important for mitigation options in managing future drought events. Therefore, it is important to examine drought impacts on vegetation and evaluate how this is simulated in models.

Drought is a frequent occurrence in southern Africa, and has enormous impacts on vegetation in the region. For instance, drought has resulted in a significant loss of biomes and death of plants (Masih *et al*., 2014, Hoffman *et al*., 2009). It is reported that there has been a significant loss of vegetation cover over the region over the last 30 years (Driver *et al*., 2012; DEA, 2015). Drought has also impacted speciation of vegetation thereby causing significant changes to the region's rich biomes, through the lack of formation of new species or even growth of species with underdeveloped morphological and physiological characteristics (Hoffman *et al*., 2009). Drought-induced vegetation loss has both ecological and socio-economic consequences on human lives. For instance, studies have shown that food security in the region is threatened due to the continual mortality of vegetation (FAO, 2000b; Müller *et al*., 2011). Other studies (e.g. Wang, 2010; Khosravi, 2017) have also reported that southern Africa could lose more than $200 billion of its GDP from the effects of drought on vegetation. The enormous impacts on vegetation have thus made it imperative to investigate how vegetation might respond to different drought intensities at varying timescales.

In order to monitor and quantify drought characteristics, drought indices are used (Wilhite and Glantz, 1985). Drought indices including the SPI (i.e. the standardized precipitation index), standardized water-level index and standardized anomaly index are derived from a single hydrological variable, which is rainfall (Kwon *et al*., 2019). Other indices such as the Palmer drought severity index, multivariate standardized drought index and standardized precipitation evapotranspiration index (SPEI) combine two or more variables related to other atmospheric or soil and environmental conditions that may predispose a plant to water stress (Palmer, 1965; Vicente-Serrano *et al*., 2010; Hao and AghaKouchak, 2013). Among the drought indices, the SPI is the most widely used because of the adjustable timescale and its relatively simple calculation (McKee *et al*., 1993). It is also recognized as appropriate for use in southern Africa (Hoffman *et al*., 2009). However, the SPI has a significant shortcoming, which is that its computation uses only rainfall without considering the effect of other meteorological variables in the development of drought occurrence (Teuling *et al*., 2013). In order to address this shortcoming, SPEI was developed for drought monitoring and it is regarded as a more suitable drought index in the region to investigate the spatiotemporal scale of drought (Ujeneza and Abiodun, 2014). SPEI is computed from the difference between potential evapotranspiration (PET) and rainfall (Vicente-Serrano *et al*., 2010). PET can be computed using different methods such as Hargreaves (HG) and Penman-Monteith (PM) method. Although studies (e.g. Vicente-Serrano *et al*., 2010) have found that PM

method captures drought better than HG, other studies (e.g. Lawal *et al*., 2019a) showed this difference is negligible over southern Africa.

Many studies have used different indices to quantify observed drought, characterize vegetation, and study drought effects on the productiveness of vegetation across different timescales. Several studies (e.g. Vicente-Serrano *et al*., 2015; Zhang *et al*., 2012; Lawal *et al*., 2019a,b) have shown that the satellite-derived normalized difference vegetation index (NDVI) is one the most important indicators of vegetation health and greenness. These studies applied NDVI in examining drought impacts on global vegetation biomes. However, other studies (Gitelson, 2004; Santin-Janin *et al*., 2009) have argued that while the NDVI is a true proxy for vegetation trends, its potential saturation makes it difficult to fully estimate biomass. In addition, because the NDVI parameters are not well calibrated and often missing in models, simulated NDVI can be biased. Due to its high correlation with NDVI, the leaf area index (LAI) is instead used to characterize vegetation conditions (Fan *et al*., 2008; Zhao *et al*., 2013). Although the LAI is an important vegetation proxy, it is rarely considered in the estimation of drought impacts on vegetation. Thus, quantifying the response of the LAI to drought over southern Africa is important for understanding the processes that modulate ecosystem services produced by vegetation which are crucial for human survival. (Melillo 2015).

Previous studies have also evaluated the performance of coupled climate models in simulating the response of vegetation to drought. For instance, Lawal *et al*. (2019a) reported that an ensemble of the Community Earth System Model (CESM) showed biases in response simulation of vegetation to drought. This was attributed to the parameterizations of the land component (i.e. Community Land Model, CLM) which poorly simulated observed NDVI. Given the poor replication of vegetation response to drought by a coupled climate model, there is a need to examine land-only models and whether they might better capture drought-vegetation relationship when the atmospheric forcings are derived from observations. The present study used Dynamic Global Vegetation models (DGVMs) to study vegetation response to drought, as little is known on how the LAI response to drought is simulated by DGVMs. The choice of DGVMs is because of their capability in simulating mostly accurate carbon exchange between the atmosphere and vegetation ecosystems (Lu *et al*., 2011).

The aim of this study is to investigate the response of LAI to droughts in southern African vegetation using observations. We also examined how well the responses are represented in model simulations. We used satellite-derived and simulated LAI to quantify vegetation responses to drought. We characterized the spatiotemporal extent of drought and its severity using the SPEI and then assessed the influence of drought using the LAI from satellite data and model simulations.

2   Data and Methodology

2.1   Data

In this study, we used satellite-calculated (hereafter, observed LAI/observation-based LAI) and simulated LAI, and satellite-derived NDVI; gridded observation and reanalysis climate datasets. The gridded observation climate datasets include precipitation, maximum, mean and minimum temperature. These data were gotten from CRU (i.e. the Climate Research Unit; Mitchell & Jones, 2005; Harris *et al*., 2014). These are global monthly data which have 0.5° x 0.5° as spatial

resolution and spans 1901 – 2019 period. Here, we used the CRU data for the period 1982 – 2011 to compute observed drought indices (i.e. SPEI) to characterize the spatiotemporal severity of drought. CRU is a gridded observed dataset, which was used because of its suitable spatial and temporal resolutions. Previous studies (e.g. New 1999; New 2000; Wolski *et al*., 2018; Otto *et al*., 2018; Harris *et al*., 2020) have shown that there is a good and robust agreement between observation network and CRU over most parts of southern Africa. We should note that sparseness and missing data generally affect the correlation between CRU and station data in the region. Furthermore, with respect to inter-annual variability, CRU robustly captures the climate factors in southern Africa. The major exception is with the long-term trend of precipitation particularly over Western Cape province of South Africa as well as wetter than normal condition over the same province. These limitations do not affect the validity of our results because we are looking at below-normal precipitation, and temperature.

The reanalysis climate data we used are the CRUJRA, which is a combination of CRU and the Japanese Reanalysis data (JRA) (University of East Anglia Climatic Research Unit; Harris, I.C., 2019). It is a 6-hourly, land surface, gridded data with a spatial resolution 0.5° x 0.5°. CRUJRA was used to compute reanalysis drought indices and used for model simulations. Here we aggregated CRUJRA to monthly samples and used the data at the same spatial and temporal resolution as CRU.

For the satellite vegetation indices, first, we used the third generation of NDVI (hereafter, NDVI3g) from the Global Inventory Modelling and Mapping Studies (GIMMS), and spans period from 1981 – 2015, with a temporal resolution of biweekly and a spatial resolution of about 8km (Pinzon and Tucker, 2014; National Center for Atmospheric Research Climate Data Guide, accessed 2019). Here, we used the data for the period 1982 – 2011. Furthermore, we used the third generation of the GIMMS LAI (LAI3g) which also spans the period 1981 – 2015 and has a temporal resolution of biweekly and spatial resolution as GIMMS3g. The LAI data had been processed (at source) using a set of neural networks which were first trained on highest-quality and post-processed MODIS LAI and FPAR products and AVHRR GIMMS NDVI3g data for the overlapping period (2000 to 2009). The trained neural networks were then used to produce the LAI3g and FPAR3g data sets (Mao and Yan, 2019). For the study, LAI3g was also used for the period 1982 – 2011. We note that GIMMS LAI and the NDVI, used in this study, are two different indices. The LAI was post-processed using different data (MODIS LAI, fPAR, AVHRR NDVI) for the period of 2000-2009. GIMMS LAI product is superior here over the GIMMS NDVI, which is due to the information derived from the MODIS LAI. The additional properties on GIMMS LAI by MODIS differentiate the index from the NDVI. Thus, it was necessary to investigate how the two indices differ. In addition, other studies (Forkel *et al*., 2013., Schaefer *et al*., 2012., Rezaei *et al*., 2016., Lawal *et al*., 2019a) have investigated how well satellite derived LAI estimate actual and ground-measured LAI.

The simulated monthly LAI data were obtained from eleven Dynamic Global Vegetation Models (DGVMs) which are part of the Trendy-version 7 (Sitch *et al*., 2008; Le Quéré *et al*., 2014). These DGVMs are CABLE-POP (Haverd *et al*., 2018), CLM (Oleson *et al*., 2013), CLASS-CTEM (Melton and Arora, 2016), DLEM (Tian *et a1*; 2015), JSBACH (Mauritsen *et al*., 2018), LPX (Lienert and Joos; 2018), OCN (Zaehle *et al*; 2011), ORCHIDEE (Goll *et al*., 2017), SURFEX (Joetzjer *et al*., 2015), JULES (Clark *et al*; 2011) and VISIT (Kato *et al*., 2013). LAI from the

models have a monthly temporal resolution spanning period from 1901 – 2017. We selected these DGVMs because they have been run with similar protocol (S3 simulations) and forcing datasets (i.e. CRUJRA).

2.2 Methods overview

2.2.1 Evaluation of DGVMs and the relationship between NDVI and LAI

The relationship between the NDVI and LAI was evaluated by computing the grid cell spatiotemporal correlation between GIMMS NDVI and GIMMS LAI. The spatiotemporal correlation between GIMMS LAI and simulated LAI from individual DGVMs was also calculated. This was necessary to show whether LAI is an appropriate estimator of NDVI, and how well the models simulate the LAI in the region. Furthermore, we made comparisons of seasonal of observed and modelled LAI. We note that the lack of available of data makes it difficult to compare GIMMS LAI and actual LAI. Nevertheless, the GIMMS LAI has been evaluated and agrees well with observations in other regions (Fan *et al*., 2019).

The climatology of observed and simulated climatic variables as well as LAI over six major biomes in southern Africa for the period 1982- 2011 were computed. These biomes are semi desert, Mediterranean, dry savanna, moist savanna, temperate grassland and tropical forest (Fig. 1; Sinclair & Beyers, 2015; Lawal *et al*., 2019a, b).

2.2.2 Description of Drought

For the present study, we adopted the definition of meteorological drought, "which is described as a period (e.g. a season) during which there is a deficit in the magnitude of precipitation in a particular area compared to the long-term normal (Palmer, 1965; Wilhite & Glantz, 1985)". The deficit in magnitude of precipitation compared to long-term normal is mostly accounted for by temperature, and less by humidity, wind or other variables. Here, we used meteorological drought because it does not make any presumptions about soil characteristics or run-off. In addition, it is acknowledged to be a primary component in the depletion of vegetation productiveness and reduction of biomass (Vicente-Serrano, *et al*., 2010). Previous studies (Vicente-Serrano *et al*., 2006; Vicente-Serrano *et al*., 2013) have also used meteorological drought in the investigation of drought impacts on biomass and vegetation productiveness.

2.2.3 Drought computation and correlation with LAI

The analyses include calculating drought (i.e. SPEI) using CRU data over a 30-year (1982 – 2011) period for different drought timescales. The drought time-scale can be described as the aggregation of temporal duration (Vicente-Serrano *et al*., 2010). SPEI is an index that is used to quantify drought (see Table 1). Therefore, the quantified values of the index give the state of drought in a space. Our definition and approaches follow numerous previous studies (Vicente-Serrano *et al*., 2013; Khosravi *et al*., 2017; Zhao *et al*., 2013; Hao *et al*., 2013).

A time series of the evolution of drought for the 30-year period was plotted. The present study extends the timeframe for understanding drought impacts from 1982 to 2011 mainly because there were frequent droughts in the 2005 – 2011 window (Masih *et al*., 2014). The timeframe was then extended back to cover a 30-year period to be long enough to cover impacts of climate change, which is particularly important considering that southern Africa experiences more frequent droughts with impacts exacerbated by climate change. This information is important for considering adaptation measures and understanding the role of climate change.

245

The drought index, SPEI, is calculated from the deduction between precipitation (P) and potential evapotranspiration (PET) as shown below:

250

$$D = P – PET…………………..… (1)$$

where D-values represent a measurement of water deficit or surplus aggregated at different time scales. D values are obtained through aggregation over individual time-scales which span 1- to 24-months (i.e. 1-, 3-, 6-, 9-, 12-, 15-, 18-, 21- and 24-month). The time-scales were calculated by including the past values of the variable. For example, a time-scale of 15-month suggests that input from the preceding 15 months, which includes the present month, was used for calculating SPEI (Begueria *et al*., 2014). "For the 1-month timescale, only the current month data is used for the calculation. The D values were standardized by assuming a suitable statistical distribution (e.g. gamma, log-logistic). The log-logistic distribution was used to standardize the D values in this study" (see also Lawal *et al*., 2019a). For more details on the timescale computation, please see Vicente-Serrano *et al*. (2010); https://rdrr.io/cran/SPEI/man/spei.html. PET is computed from maximum temperature, minimum temperature and mean temperature, using Hargreaves technique (e.g. Vicente-Serrano *et al*., 2012; Begueria *et al*., 2014; Stagge *et al*., 2014).

255

260

265

We note that the PET in the SPEI was computed using Hargreaves (HG) method rather than Penman-Monteith (PM) because the data (e.g. vapour pressure, maximum and minimum humidity) required for computing PM over southern Africa are sometimes missing or not available at the needed gridded spatial resolutions and timespan. Although PM is considered better in most regions, Lawal *et al*. (2019a) showed that the variation between the PM and HG is negligible for southern African region. The study only considered observed SPEI_PM which was obtained from https://spei.csic.es/database.html and not modelled SPEI_PM due to the unavailability of simulated data required for its computation. Other studies (e.g. Begueria *et al*., 2014) have also found that there is an insignificant contrast in the strength of PM and HG for reproducing their divergence on measured variables such as vegetation indices. We should also note that the SPEI (unlike SPI or PDSI) is the most appropriate index for measuring drought in southern Africa, as it accounts for the effect of evaporative demand from the atmosphere in drought monitoring (Vicente-Serrano *et al*., 2010; Ujeneza *et al*., 2014). In addition, the SPEI is reported to be able to identify the geographical and temporal coverage of droughts (Vicente-Serrano *et al*., 2010; Ujeneza *et al*., 2014).

270

275

280

285

Table 1. Definition of drought thresholds based on the SPEI scale

SPEI	Drought thresholds
2 or more	Extreme wet
1.5 to 1.99	Severe wet
1 to 1.49	Moderate wet
0 to 0.99	Mild wet
0 to -0.99	Mild drought
-1 to -1.49	Moderate drought
-1.5 to -1.99	Severe drought
-2 or less	Extreme drought

Source: Wang *et al*. (2014), modified as shown in Lawal, 2018.

290 We deseasonalized GIMMS LAI by transforming monthly LAI series per pixel to symbolize the standardized deviations from extended mean. This was to make the sequence of LAI commensurate to SPEI (Vicente-Serrano *et al*., 2013) and eliminate the impact of periodicity on vegetation response. We note that the SPEI is intrinsically deseasonalized.

295 In order to reconcile the difference in spatial resolutions of CRU and GIMMS, we regridded the data to the same spatial resolution using the bilinear interpolation method. We then computed the correlation per grid-cell between SPEI (based on CRU) and deseasonalized LAI over the 30-year period at the different drought timescales using Pearson correlations. We then compared the spatial distribution of maximum (peak) correlation and the comparable time-scales of drought for

300 observed SPEI. Our analyses consider the periods which LAI responds to the presence/absence as well as the severity of drought. This is referred to as "drought time scale" in the study.

Next, we investigated correlations at each grid cell between the drought (from reanalysis - CRUJRA) and an ensemble median of deseasonalized modelled LAI from individual DGVMs.

305 The peak (maximum) correlations and equivalent time-scales from the complete 1- to 24-month time-scales were mapped for the ensemble median over the 30-year period. We used ensemble median because of its less sensitivity to independent outliers (Reuter *et al*., 2013). In summary, we calculated model ensemble drought from the median from individual members' drought indices. The inter-annual variation of drought impacts on LAI by individual DGVM was also calculated

310 for different timescales. We also examined the observed and an ensemble mean of simulated LAI response to drought across latitudes.

In summary, CRU was used to compute observed drought while CRUJRA was used to calculate modeled drought because it is what was used to force the models. This will allow for easy

315 observation and model comparisons.

Similar to Lawal *et al*., 2019a, we calculated the seasonal mean for four seasons i.e. a) December-January-February (DJF); b) March-April-May (MAM); c) June-July-August (JJA); and d) September-October-November (SON) from the correlations of monthly series of drought and LAI.

320 These were computed from correlating monthly series (twelve series per year) per pixel of

GIMMS-LAI and each monthly series of 1- to 24-months drought (SPEI) series over the 30-year period with Pearson correlation. The same technique was used for the model ensemble. In simpler terms, we calculated the correlations (twelve sequences in a year) of monthly LAI to monthly sequences of 1- to 24-months SPEI using 30-years of data. Subsequently, the seasonal mean of these correlations was calculated. The peak correlations and drought timescales of the models were calculated over six major biomes in southern Africa, namely (Fig. 1) – Temperate grassland, Tropical forest, Moist Savanna, Dry Savanna, Semi-desert and Mediterranean vegetation. These regions were selected because of their relative importance and are most affected by drought.

Finally, the impacts of extreme events (wet and dry years) at different time periods were compared; and the comparison of global and regional responses to drought across biomes for the period 1982 – 2011 was investigated.
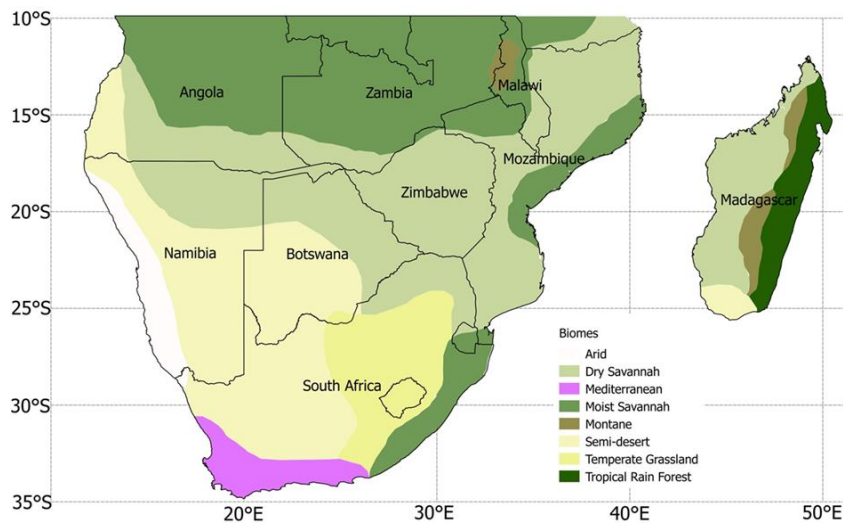
Figure 1. Major vegetation biomes in southern Africa (adapted from UNEP, 2008, Sinclair & Beyers, 2015 and Lawal *et al.*, 2019a,b). The black lines indicate political boundaries.

3   Results

3.1   Grid cell correlations between NDVI and LAI

Figure 2 illustrates the relationships between the NDVI and LAI for observations, as well as the comparison between observed and model LAI. There is a strong linear relationship between observed NDVI and LAI (Fig. 2a). The correlation (0.94) is high between both variables and the standard deviation is low (0.005). The standard deviation being referred to is for GIMMS LAI and individual DGVMs, as well as GIMMS LAI and GIMMS NDVI. From the figure, there is a log-

like shape, where NDVI grows faster when LAI is low (<0.2) and becomes saturated when LAI goes higher (>0.3). A linear regression of the data shows a slope of 2.15. The low standard deviation indicates that the values from the two indices are close. Although there is a good agreement between observed NDVI and LAI, the 1:1 line shows that the datasets are not exactly equal.

Furthermore, there is good agreement between observed and the simulated LAI (Fig. 2). JULES has the highest correlation (0.97) with observation (Fig. 2l). CLM has the weakest (0.73) correlation with the observations (Fig. 2c). DLEM and LPX have the same correlation coefficient value of 0.87 with observation (Fig. 2e, 2g). The positive relationships between simulated and observed LAI indicate a general applicability in investigating the model's performance of vegetation response to drought. It also shows that the correlation is strong enough to compare how the LAI reacts to drought in the ensemble. An aggregation of observation along the gradient of simulated LAI shows that most of the models have similar slopes with observation.
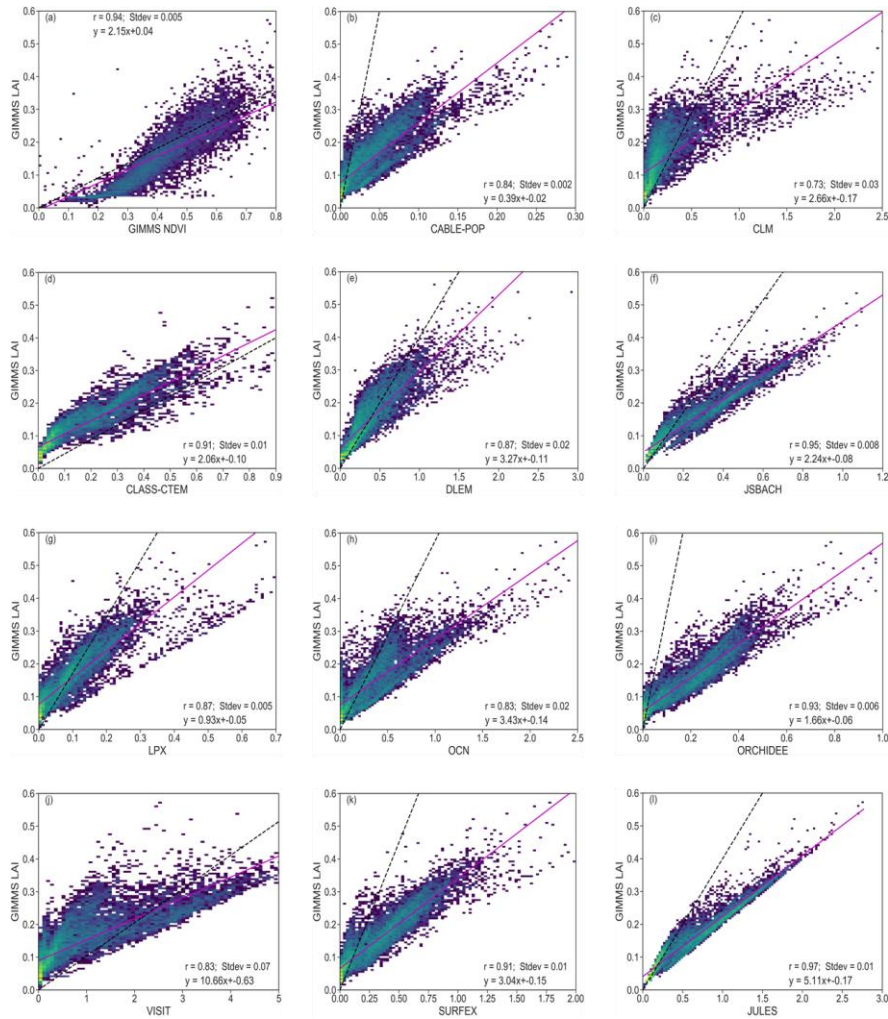
365

Figure 2. Scatterplots of correlations between vegetation indices (observation and model) for the period 1982 – 2011 over southern Africa. Inset values indicate the correlation coefficient (r) and standard deviation (Stdev) between GIMMS LAI and GIMMS NDVI, as well as GIMMS LAI and modelled LAI. The colour represents each grid cell. The pink solid line is the linear regression, while the dashed black line shows 1:1 line. The unequal x-axes are to visualize the detailed data for the models.

370

375

3.2   Seasonal and interannual variations of observed and modelled LAI

The comparison of seasonal and interannual variation of observed and modelled LAI is given in Fig. 3. The model shows a stronger positive bias in JJA and SON in comparison to summer and winter months; and a negative bias over the tropical forest region of Madagascar (Figs. 3A – 3D). In addition, model mostly overestimate the seasonal patterns of LAI in some regions during DJF and JJA, and underestimate LAI in MAM and SON (Figs. 3E – 3L). Over most parts of the region, there is a strong correlation and good agreement between observed and modelled LAI in DJF, MAM and JJA although it is weaker in SON (Figs. 3M – 3T). The strong correlation is more prevalent in JJA than other seasons (Fig. 3S); while it is weakest in southern parts of the region. However, the correlation is largely negative over Angola in DJF and SON (Figs. 3Q, 3T). Furthermore, the correlations between model and observed LAI is weaker in deseasonalized data (hereafter, Deseas. Correlation; Figs. 3M– 3P) than in original data (hereafter, ORIG. Correlation; Figs. 3Q– 3T), thereby showing the effects of seasonal patterns on time-series data. With respect to the period, 1982 – 2011 (hereafter, ANNUAL), the correlation between modelled and observed LAI are different for deseasonalized and original data (Figs. 3U – 3V). For the former (Fig. 3U), there is gradient in the correlation across the region, with higher values in central and southern parts than in Angola and Madagascar. However, with the original LAI data (Fig. 3V), the correlation is very high (about 0.85) and more prevalent, except in eastern Madagascar and Western Cape Province of South Africa.
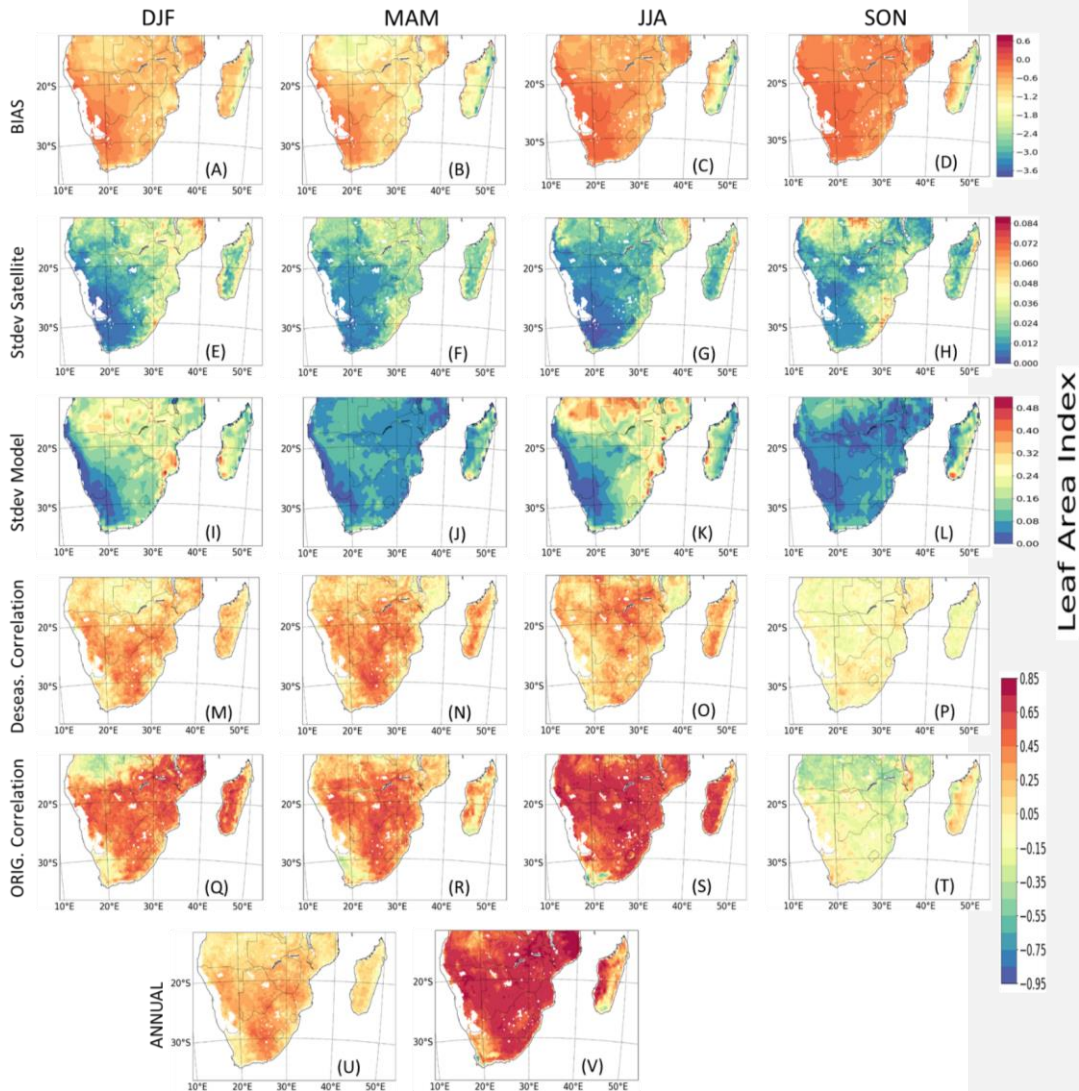
Figure 3. Spatial seasonal distribution and inter-annual variability (IAV) of satellite-calculated and modelled LAI (multi-model mean) over southern Africa. (A) – (D) show the difference (bias); (E) – (H) and (I) – (L) show their standard deviation (Stdev); (M) – (P) show the correlations between deseasonalized GIMMS LAI and modelled LAI; (Q) – (T) show their correlations for original GIMMS LAI and modelled LAI and (U) – (V) show correlations between GIMMS LAI and modelled LAI but for the period 1982 – 2011. The inter-annual variability for observed and modelled LAI for the period 1982 – 2011 is shown in Fig. S8.

3.3   Climatology of observed and, simulated climate variables and LAI

This section compares the seasonal cycle of observational (CRU and CRUJRA) climate variables; as well as observed and simulated LAI from GIMMS LAI and TRENDY models, respectively. Precipitation and temperature are seasonally variable and their climatologies are mostly similar. For example, precipitation is higher in MAM and DJF over many of the biomes except in Mediterranean vegetation where precipitation is higher in JJA (Figs. 4a, 4d, 4g, 4m, 4p). The wettest month occurs over TF (i.e. tropical forest biome) where the precipitation is about 350mm. Conversely, during the dry season (JJA), there is little rainfall in the biome, although, it experiences some precipitation June and July. Over the Mediterranean vegetation (Fig. 4j), a winter (JJA) rainfall region, rainfall variability is lower and is mostly dry in the DJF and SON. Similarly, the highest minimum and maximum temperature in the region is observed in the DJF season, where the highest temperature value exceeds 30°C. Over the tropical forest biome, although the distribution pattern of precipitation and temperature are similar for most months, they differ during June and July months. The pattern of precipitation and temperature distribution generally differ over the Mediterranean vegetation. The pattern of temperature and precipitation from CRUJRA follows CRU, although the ensemble spread is much narrower (Fig. 4c, 4f, 4i, 4l, 4o, 4r). The spatial patterns of the climate variables from CRU and CRUJRA are shown in Fig. 5. CRUJRA well simulates the pattern of precipitation over southern Africa (Figs. 5a and 5b) as CRU although it shows some biases in magnitudes, as well as for minimum temperature (Figs. 5g and 5h).

There is not strong seasonality for LAI, with maximum observed LAI values less than 4 in all biomes. The models well reproduce the climatology of LAI over the southern African biomes with a few exceptions (Figs. 4b, 4e, 4h, 4k, 4n, 4q). For instance, the models simulate the drop in LAI over the semi desert, temperate grassland, tropical forest, dry savanna and moist savanna biomes in JJA. The highest increase in observed LAI occurs over the tropical forest in April, although the models simulate a decrease in LAI over tropical forest during this time. On the other hand, lowest amount (less than 0.1) of LAI is observed in September and this occurs over the semi-desert biome. Observations typically fall within the range of the model ensemble. In addition, the distribution pattern of simulated LAI is similar to observation in most biomes except in the Mediterranean and tropical forest biomes. The LAI pattern also follows that of the climatic variables although the former lag. The lag effect is accounted for in this study, and is known as drought time scale.
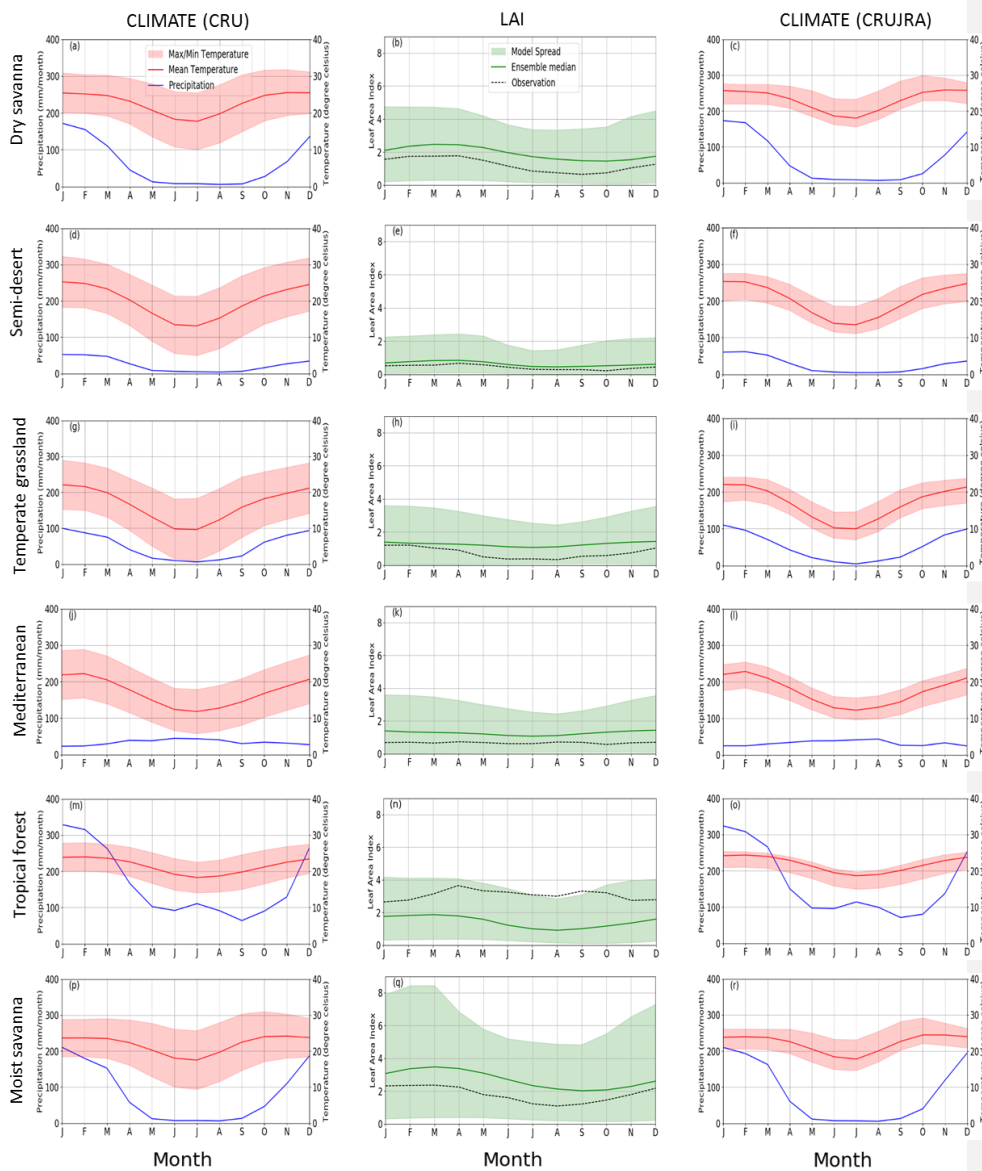
445 Figure 4. Annual cycle of observed climate variables (precipitation, mm/month; maximum, minimum and mean temperature, ºC) and LAI for observation and multi-model mean (TRENDY) across six southern African biomes over for the period 1982 – 2011. The annual cycle of the LAI for individual models are shown in Figure S5.
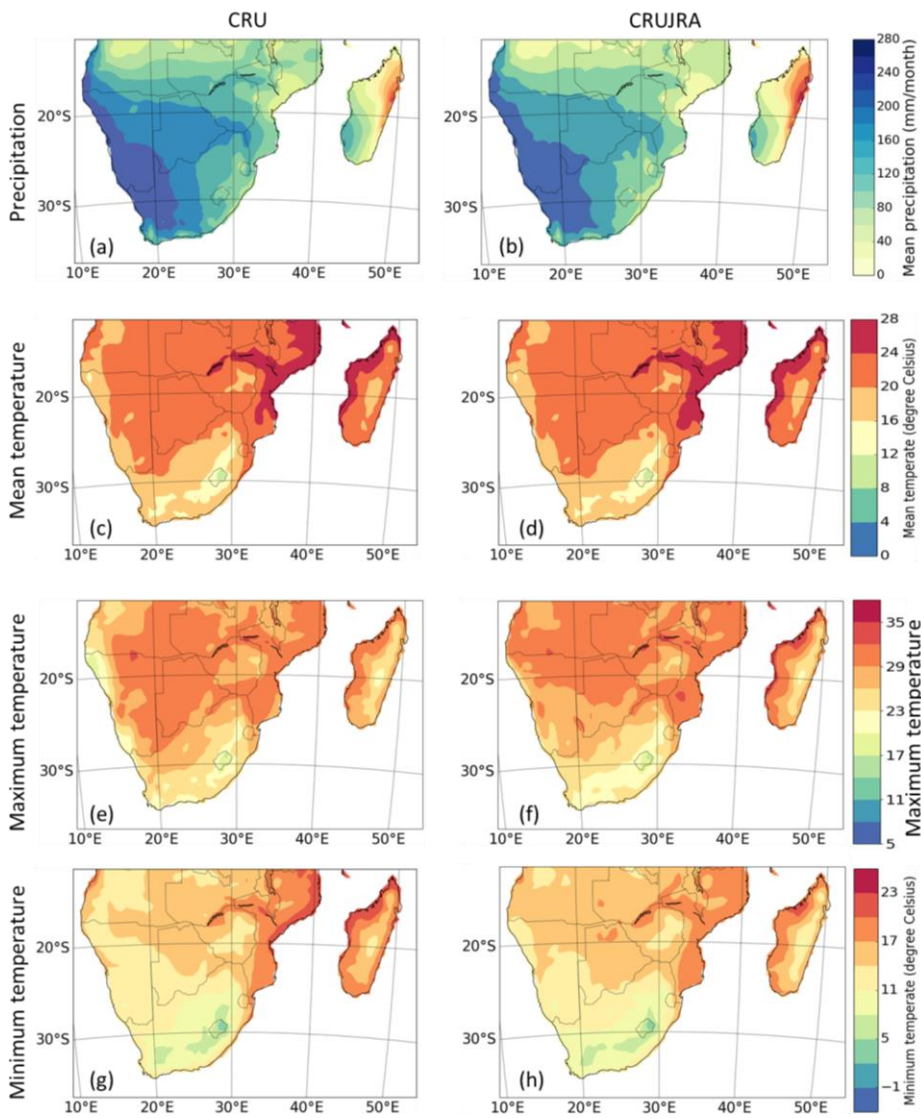
Figure 5. Spatial distribution of precipitation, mean temperature, maximum temperature and minimum temperature over southern Africa in CRU and CRUJRA; for the periods 1982 – 2011.

450

455

3.4 The evolution of drought in southern Africa

Figure 6 shows the evolution of observed SPEI in southern Africa between 1982 and 2011. Here, drought indices from CRUJRA are not included because preliminary investigation showed close magnitudes for drought indices computed from CRU and CRUJRA. We note that CRU was used to calculate SPEI for observation while simulated SPEI was computed with CRUJRA.

There is inter-annual, seasonal and decadal variability of the drought indices during dry and wet conditions over southern Africa. Although 1-, 3- and 6-month SPEI indicate no trend in wet or dry spells, they show the intensity of drought event for the 30-year period (Figs. 6a, 6b, 6c). The highest magnitude of drought is captured by 1-month SPEI while the lowest is shown in 21-month SPEI. The severity of drought intensity is similar for all SPEI (i.e. 1-month to 24-month SPEI). The magnitude of the severity is on the y-axis of 1-month to 24-month SPEI.

We note an increasing trend in SPEI (9- to 24-month). Tables 2 and 3 illustrate when droughts occurred, as well as the severity of drought within the 30-year period. They also show, however, that droughts were most frequent and intense in the second decade, thus, indicating how climate change is expected to increase the frequency and severity of droughts.
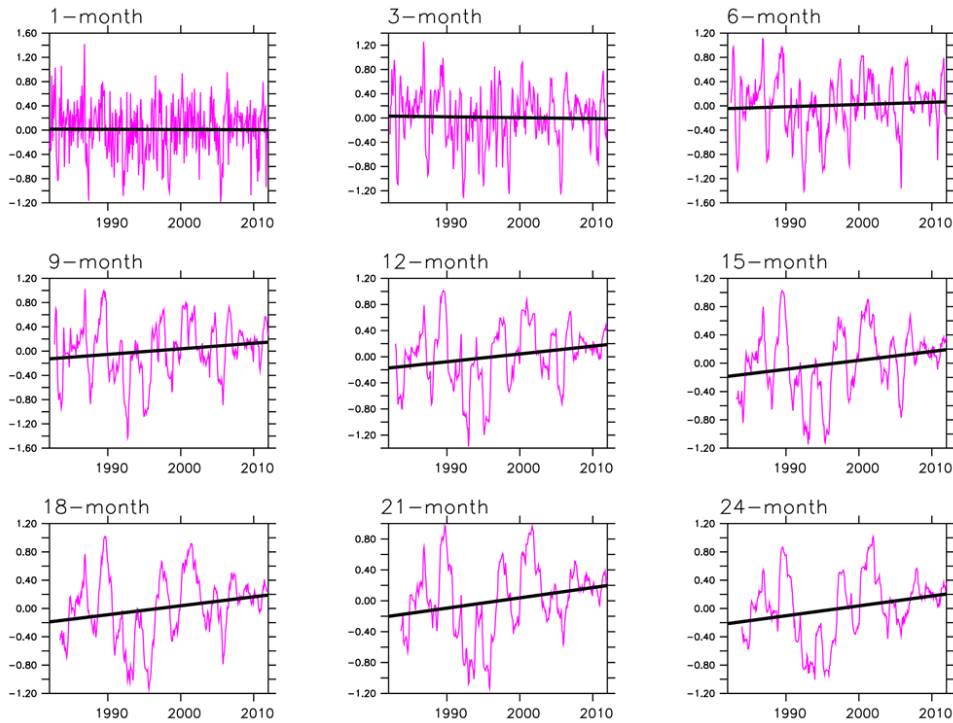
Figure 6. Evolution of SPEI in southern Africa for the period 1982 – 2011. The trend is significant at 90% confidence interval for all timescales.

480

Table 2. Characteristics of drought occurrence for 1- to 24-month drought timescale for 1st decade (1982-1991), 2nd decade (1992-2001) and 3rd decade (2002- 2011).

Drought Timescale	Number of drought events			Year of moderate drought events		
	1st Decade	2nd Decade	3rd Decade	1st Decade	2nd Decade	3rd Decade
1-month	53	62	53	1987	1992, 1990	2004, 2007, 2008, 2011
3-month	55	64	58	1988	1991, 1992	2004, 2008, 2011
6-month	44	62	60	1982	1992, 1993	2004
9-month	55	66	62	-	1992, 1994	-
12-month	53	68	56	-	1992, 1995	-
15-month	58	63	56	-	1992	-
18-month	54	69	51	-	1992, 1994	-
21-month	51	69	56	-	1992, 1995	-
24-month	41	71	54	-	1992, 1994	-

Table 3. Statistics of the severity of drought for 1- to 24-month drought timescale for 1st decade (1982-1991), 2nd decade (1992-2001) and 3rd decade (2002- 2011). SD is the standard deviation and Max is the highest magnitude of drought occurrence.

Drought Timescale	Mean			SD			Max		
	1st Decade	2nd Decade	3rd Decade	1st Decade	2nd Decade	3rd Decade	1st Decade	2nd Decade	3rd Decade
1-month	0.30	0.39	0.31	0.26	0.26	0.27	1.1	1.02	1.15
3-month	0.32	0.36	0.29	0.24	0.25	0.25	1.02	1.01	1.12
6-month	0.38	0.38	0.26	0.31	0.28	0.24	1.04	1.3	1.33
9-month	0.31	0.41	0.21	0.26	0.35	0.18	0.86	1.32	0.83
12-month	0.30	0.43	0.21	0.21	0.35	0.18	0.81	1.27	0.7
15-month	0.28	0.47	0.20	0.21	0.31	0.18	0.77	1.13	0.7
18-month	0.27	0.48	0.20	0.17	0.28	0.12	1.02	1.02	0.77
21-month	0.18	0.50	0.17	0.2	0.28	0.14	0.62	1.00	0.61
24-month	0.28	0.51	0.15	0.19	0.24	0.11	0.55	0.93	0.46

3.5   Spatial distribution of LAI response to drought and the timescales

Figure 7 presents the spatial distribution of the peak correlation between the SPEI and the LAI, and the timescales at which the correlation occurs. This is to show the magnitude of response of LAI to drought in southern Africa, and the length of the period for the response.

Observations show that southern African LAI can respond fairly strongly to droughts (peak correlation magnitudes of between 0.4 and 0.6), though the response is much weaker ($r < 0.4$) in eastern Madagascar, Angola and parts of South Africa (Fig. 7a). The TRENDY multi model median generally overestimate the observed magnitude of the LAI to drought response (Fig. 7c). Peak correlations for the models seem to be much stronger – in the 0.6-0.8 range for most of the regions. In addition, over the arid areas of Namibia, models simulate a LAI while observations depict no measurable LAI, indicating that models simulate the LAI in areas where observations show no measurable LAI.

The multi model median have a drought timescale that is mostly longer than the observations (Figs. 7b, d). For instance, drought response of simulated LAI occurs mostly over a longer time period (6-, 9-month timescale) than in the observation over eastern Madagascar. Over southern areas of Madagascar and central Zambia, the multi model median overestimates the drought timescale. Over central areas of South Africa and Mozambique, simulated LAI responds at intermediate (9-month) timescales. In comparison, similar drought timescales for the observation and the model ensemble median are shown in parts of Angola.
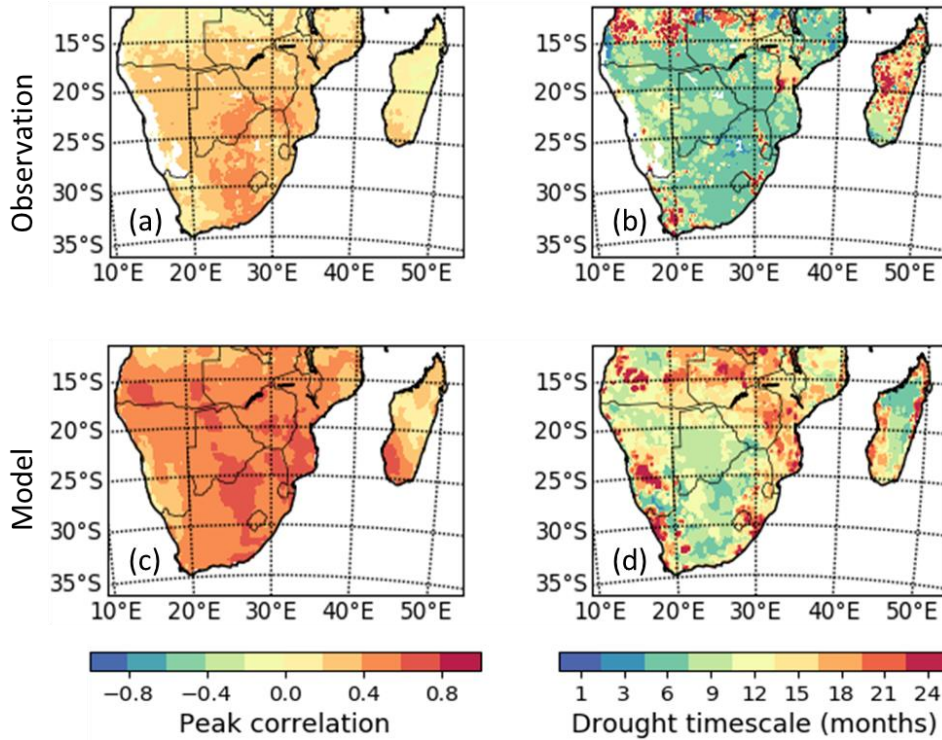
Figure 7. Spatial distribution of peak correlation between drought (SPEI) and LAI over the region of southern Africa in the observation and in the model ensemble median; for the period 1982 – 2011. Panels (a) and (c) show the peak correlation per pixel, which is independent of the timescale and the month of the year. Panels (b) and (d) indicate the timescales at which the peak correlation between SPEI and LAI is found. Areas with no significant correlation are white.

3.6   Latitudinal distributions of LAI response to drought and the timescales

The present study investigated and discussed the implications of drought on different vegetation/biome types across latitudes in the region. Here, we stratified the LAI response to drought based on latitude, because we intend to investigate and identify the shift in response based on the vegetation types across the latitudinal belt.

While the pattern of the latitudinal distribution of the LAI response to drought is identical across different timescales, the magnitudes generally differ (Fig. 8). The response is much weaker (less than 0.15) for the 1-month timescale than for other timescales. The strongest response is observed at 6-month timescale between latitudes 25 and 30°. The model ensemble mean generally agrees with the pattern of the observed LAI-SPEI correlations across all the timescales. However, the

magnitudes differ from the observation. Modeled correlation is stronger than observations for the longer (6-month or more) timescales. This means that the models are oversimplifying how LAI responds to drought by neglecting other climate factors, such that in models, LAI only correlates to water deficit (SPEI). Furthermore, there is an offset between observation and model mean which is consistent across most of the timescales, perhaps due to strong memory of the some of the models.
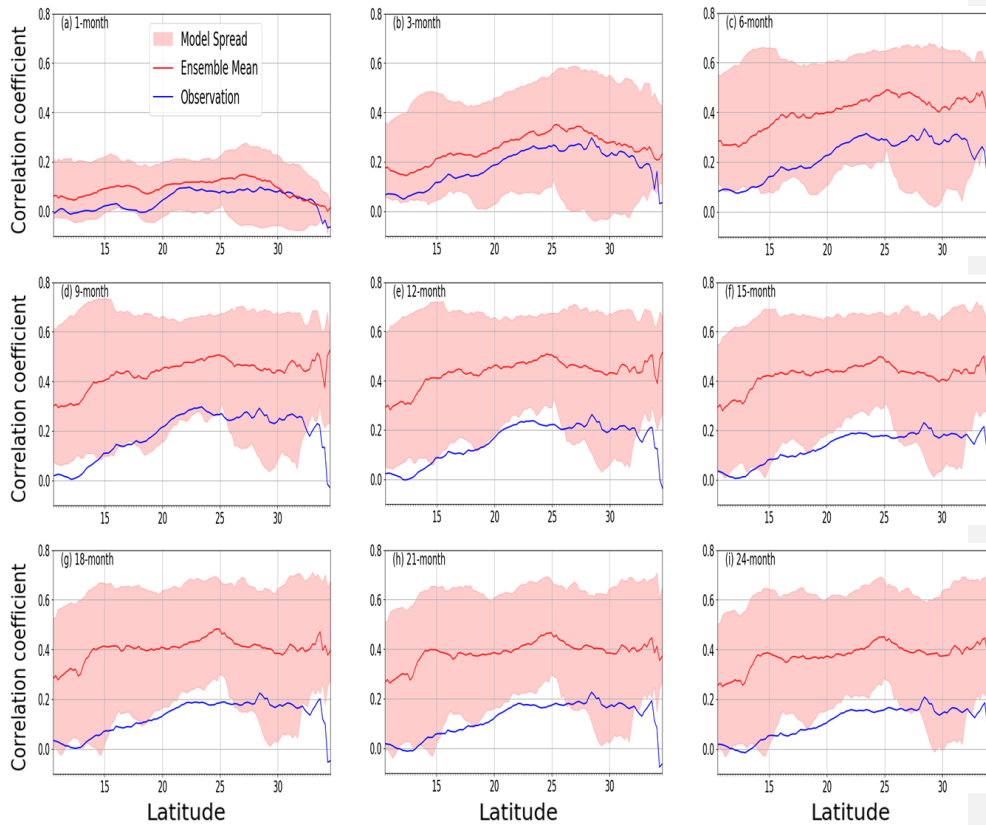
Figure 8. Mean correlation (observed and multi-model ensemble) of annual LAI and SPEI for 1982 – 2011 across latitudes over southern Africa for 1- to 24-month timescales.

3.7   Response of LAI to droughts across seasons

Observations show similar correlations between LAI and drought across all seasons in the biomes (Fig. 9). For the dry savanna, which is one of the most climate-impacted biomes in the region, LAI

response to drought is strong and the correlation is as high as 0.8 in MAM season and it occurs at 12-month timescale. The correlations between drought and LAI are also very strong in other seasons over the same biome and occur at 6- and 12-month drought timescale, except over the Mediterranean vegetation where the response occurs at 18-month in DJF season. Similarly, the peak correlations between drought and LAI are strong across the other biomes. With an exception of the tropical forest biome, the drought timescale is at longer time periods (> 6-months).

The model ensemble generally overestimates correlations across the biomes in different seasons. Whilst the correlation magnitude remains mostly larger than observation, nonetheless, models simulate closer correlation with observation in some biomes and seasons. For instance, over Mediterranean vegetation, models simulate fairly good response of LAI to drought in all seasons. Furthermore, in nearly all other biomes, the ensemble spread overlaps with the observations. In addition, simulations mostly overestimate drought timescale, except over dry savanna. A possible reason for the difference why the time scale for Dry savanna was underestimated may be because phenological triggers for dry savannah vegetation types respond differently to environmental variables, which the models do not capture. The African Dry savanna region is characterized by rapid vegetation changes due to fire, land-use among others, as well as senescence for prolonged dry periods (Rahimzadeh-Bajgiran *et al*., 2012; Zhu and Liu, 2015), which may have contributed to the underestimation in the response of the models. Similarly, models have different representations of fire, which could also indirectly contribute to the underestimated model responses to drought.
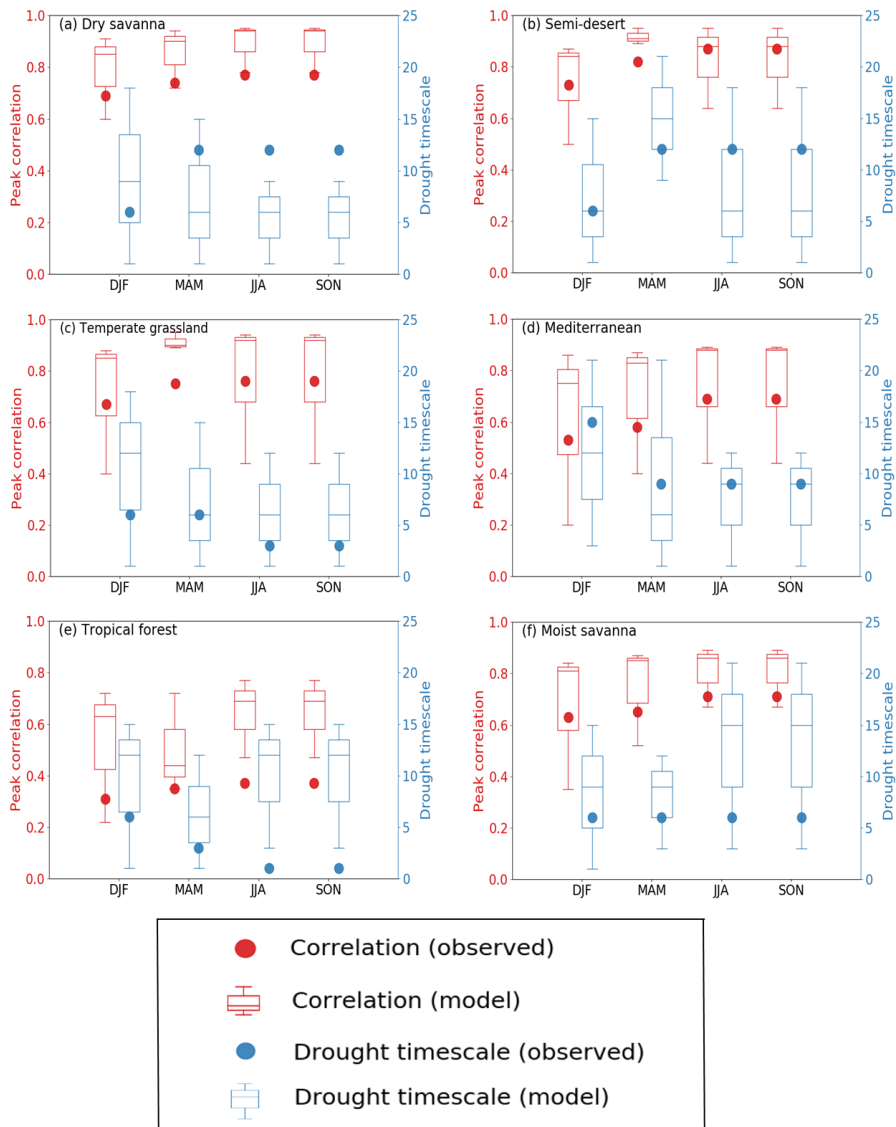
Figure 9. Seasonal correlations of drought (SPEI) and LAI across six southern African biomes.
590 The values on the left axis show the peak correlation in observation and TRENDY models. The
values on the right axis indicate the corresponding drought timescale.

3.8   Inter-annual variation of model simulation of drought impacts on LAI

Table 4 shows the correlations between observed mean SPEI and LAI for the period 1982 and
2011 as well simulations by individual DGVM across different timescales. Unlike Fig. 7 which
shows the peak correlations, the table shows the mean correlation for the 30-year period.

There is variation in the inter-annual simulation of LAI response to drought across different
timescales by individual models. For instance, on the 1-month timescale, JULES simulates the
least correlation value while JSBACH shows the highest correlation value. Furthermore, JSBACH
simulates the highest correlation value for most of the timescales while CLM simulates the least
correlation values for most (3-, 9-, 12-, 15- and 18-month) of the timescales. A possible reason for
the weak performance of CLM may be its representation of the canopy construction of the PFTs
and of its foliage clumping representation. In addition, CLM is limited in its simulations of
vegetation with regards to transpiration, due to rooting depth among others (Dahlin *et al.*, 2020).
Furthermore, CLM does not well simulate savanna ecosystems, but instead uses a combination of
grasses, shrubs, and trees. There are also some problems (such as an unusual green-up in dry
season) identified with stress deciduous responses (Dahlin *et al.*, 2015).

Table 4. Model simulation of mean SPEI and LAI correlations between 1982 and 2011. * indicates
the model with the lowest mean correlation.

Correl.	GIMMS LAI	CABLE-POP	CLM	CLASS-CTEM	DLEM	JSBACH	LPX	OCN	ORCHIDEE	SURFEX	JULES	VISIT
1-month	0.0066	0.1017	0.1188	0.1266	0.085	0.1388	0.0842	0.0579	0.0884	0.1094	0.027*	0.086
3-month	0.0775	0.3084	0.0187*	0.29	0.2499	0.4165	0.2403	0.1644	0.266	0.2791	0.1434	0.1108
6-month	0.091	0.3474	0.1806	0.3562	0.3305	0.5404	0.2386	0.3377	0.3733	0.3759	0.2429	0.1703*
9-month	0.0832	0.333	0.2034*	0.3496	0.3437	0.5734	0.2505	0.4055	0.39	0.3994	0.3189	0.23
12-month	0.0813	0.3053	0.2155*	0.3231	0.3229	0.5398	0.304	0.4109	0.4054	0.3911	0.3663	0.2892
15-month	0.0642	0.2773	0.2161*	0.2912	0.2846	0.4925	0.3208	0.4106	0.4132	0.3547	0.3623	0.3198
18-month	0.0452	0.2534	0.2349*	0.276	0.2381	0.4599	0.2405	0.3998	0.4109	0.3289	0.3586	0.3472
21-month	0.0406	0.239	0.2402	0.27	0.2119	0.4334	0.1569*	0.3739	0.3962	0.2955	0.3621	0.3501
24-month	0.0409	0.2302	0.2355	0.2668	0.2186	0.4696	0.2064*	0.3528	0.3777	0.2682	0.3617	0.327

3.9 Impacts of extreme events on LAI

The impacts of extreme events on LAI are shown in Fig. 10. The objective was to discuss the impacts and compound influences of extreme events on LAI during extreme hot/dry and wet years. Here, extreme events are the wet (2000, 2010, 2011) years - i.e. the periods with precipitation higher than normal; and the dry (1983, 1984, 1991) years which include the periods of very high dry spells. To achieve this, we used the anomaly of precipitation, SPEI and LAI relative to the long-term mean. The anomaly was computed as a difference between a particular extreme dry or wet year and 30-year mean representing dry and wet conditions. The anomaly is the magnitude of impacts added by the extreme event in a particular year. The spatial pattern of the changes in LAI, SPEI and precipitation were then plotted. Our analyses follow Pan *et al*. (2015). Furthermore, we computed the pattern correlation coefficients (r) between the LAI and climate variables for each extreme dry and wet year. The statistical significance of the coefficients was also calculated. The goal of this is to ascertain whether the sign of anomaly of the variables correspond in the same locations on two different maps. In order to determine the significance of correlation coefficient, we performed the Linear Regression T-Test (i.e. LinRegTTest). This finds the best line of fit among a set of data points. It also checks the quality of the fit by carrying out a t-test on the slope, thus testing the null hypothesis that the best fitted line is 0, suggesting that there is no correlation between two variables, since an association with a slope of zero implies that one variable does not affect the other. Therefore, if the *p*-value is not sufficiently low, then we do not have sufficient data to accept relationship between the variables. For this study, we used a significance level of 5% i.e. $\alpha = 0.05$, which is the most commonly used value in life and biological sciences. We then tested the hypothesis on whether the *p*-value is less than the significance level ($\alpha = 0.05$), which is our null hypothesis. In cases where that is the case, we rejected the null hypothesis and concluded that there is adequate evidence that there is a significant linear relationship between the variables i.e. LAI-SPEI and LAI-Precipitation. In cases where *p*-value is greater, we do not reject null hypothesis since there is not enough evidence to conclude on the significance of correlation coefficients.

Note, although the SPEI is a drought index, it was also considered in a wet year because the impact of drought usually lasts beyond a dry year especially in semi-arid regions of southern Africa. In addition, hot temperature has an influence on the worsening of drought by causing water to evaporate from the soil. SPEI, as a drought index, considers temperature effects on moisture availability.

We considered only observation i.e. CRU (precipitation and drought) and satellite-calculated LAI. The observed climate (CRU) data are not sub-monthly. Only the CRUJRA (reanalysis), which was used for model correlation, is sub-monthly. Model was not analyzed in this section because our goal was simply to examine the observed impacts (or influence) of an extreme event.

The spatial pattern of change of LAI and SPEI are mostly similar during extreme dry and wet years (Fig. 10). For example, in 1983 (a dry year), the negative anomaly of LAI in some parts of the region largely follows the negative anomaly of the SPEI, except in western and central parts. (Figs. 10A & 10B). In 1984, both variables show a strong positive anomaly over Madagascar, Swaziland

and Kwazula Natal Province of South Africa (Figs. 10D & 10E). The pattern of change of both SPEI and LAI are also comparable during extreme wet year. In the wet year of 2000, the positive anomaly of SPEI that is observed in Nambia and South Africa is also evident for the LAI (Figs. 10J & 10K). In a like manner, both variables show negative anomaly over Malawi and Zambia. The strongest pattern (magnitudes) of change of the SPEI in the region is observed in the dry year of 1991 (Fig. 10H). However, the pattern of change of the LAI and SPEI are not similar over some regions in some periods. For instance, in 1991, while a negative anomaly of the SPEI is observed in northern Madagascar and central parts of southern Africa, LAI shows a positive anomaly (Figs. 10G and 10H). The opposite and decreasing relationship between the two variables in 1991 is also evident in the pattern correlation coefficient value of – 0.16 (Fig. 10H). The variation in anomaly in these parts and period may be due to the exertion of stronger influence by other factors such as residual soil moisture and precipitation (see Fig. 10I), with temperature having negligible impacts.

The influence of precipitation (as a standalone meteorological factor) on LAI during extreme events is limited. This is observed from the disparity in the spatial pattern of the LAI and precipitation over some regions and periods. For example, in 1984, the wide negative anomaly of precipitation that is shown over Zimbabwe, Mozambique and southern Madagascar is opposite to the LAI, which shows positive anomaly (Figs. 10D and 10F). The LAI anomaly is more similar to that of the SPEI (Fig. 10E). Also, in wet year of 2000, while precipitation shows preponderant increase over northeastern parts of southern Africa, there is a decrease in the LAI as is the case with SPEI (Figs. 10J – 10L). Nevertheless, precipitation plays a primary/major role in the pattern of change of LAI, as is observed over the most parts of the region during the years considered.

Generally, the pattern correlation coefficient values between the LAI and SPEI are higher than those between the LAI and precipitation in extreme dry and wet years (Table 5). Although the coffiecients are small, they are mostly significant across the different extreme periods, except for 1983, an extremely dry year, where the p-value is 0.58, for LAI-SPEI (Table 5). The extremely low statistical significance indicate low standard errors and large number of gridsizes for the region.
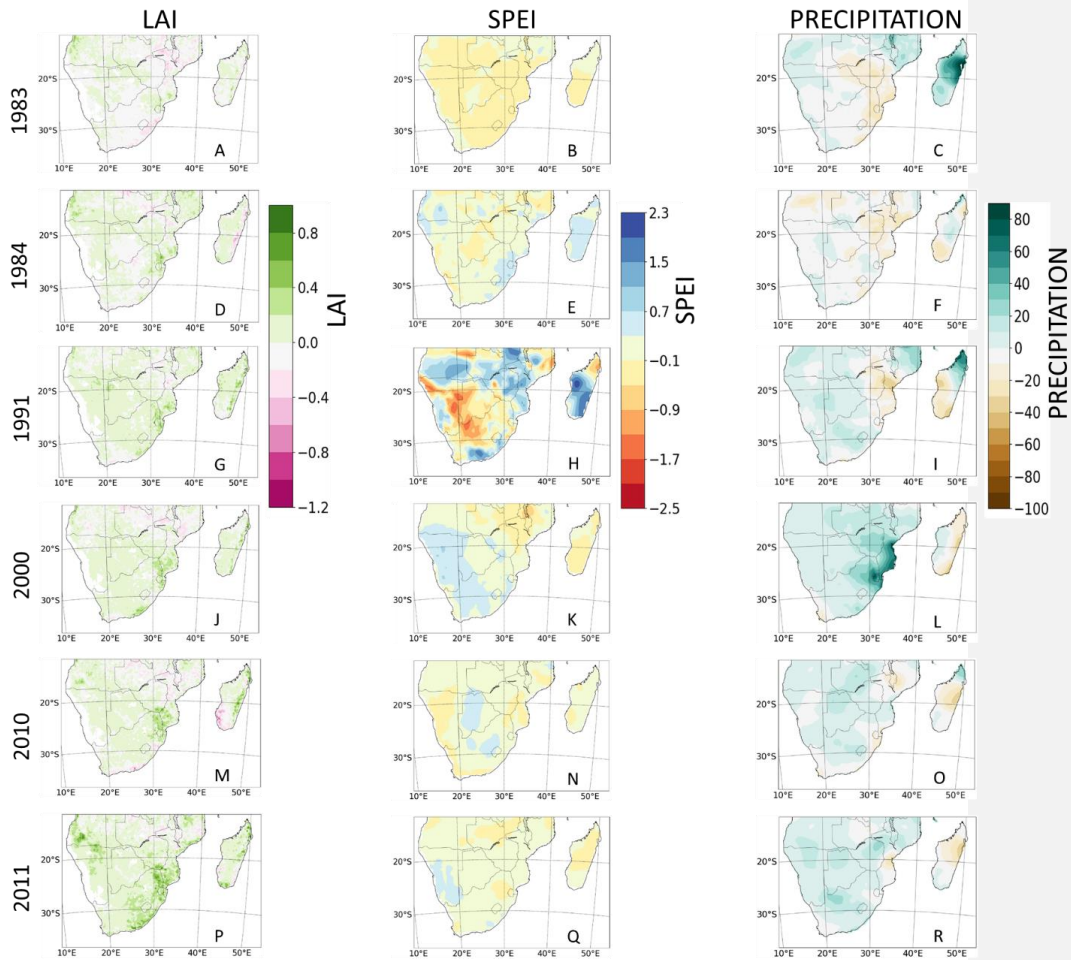
Figure 10. Spatial pattern changes in satellite-calculated LAI, observed SPEI and precipitation during extreme dry (1983, 1984, 1991) and wet (2000, 2010, 2011) years. For (A) – (I), the changes in LAI, SPEI and precipitation were calculated as a difference between the dry year and the 30-year mean, and for (J) – (R), changes in LAI, SPEI and precipitation were calculated as the difference between the wet year and the 30-year mean. White areas indicate no correlation. The pattern correlation coefficients and the statistical significance of the coefficients between the variables are given in Table 5.

Table 5. Pattern correlation coefficients (r-values) and significance of the coefficients calculated at significance level of 5% ($\alpha = 0.05$) between the LAI and SPEI, for extreme dry and wet years; as well as between the LAI and precipitation during extreme dry and wet years. The correlation coefficients are significant when *p*-value is less than 0.05.

Year	LAI – SPEI		LAI – PRECIPITATION	
	r-values	p-values (0.05)	r-values	p-values (0.05)
1983	0.1	0.58	-0.02	2.43E-06
1984	0.17	7.09E-64	0.04	8.33E-05
1991	-0.16	1.1E-41	0.16	9.83E-60
2000	0.23	1.5E-121	0.14	2.81E-27
2010	0.14	6.3E-17	0.1	0.008
2010	0.14	2.2E-48	0.1	1.47E-06

3.10 Comparison of global and regional distribution of LAI response to droughts (1982 – 2011)

There is variability in the global and regional temporal distribution of LAI response to drought (at 12-month timescale) when global vegetation biomes are split into regional biomes (Fig. 11). The map of the global biomes is shown in Fig. S1 in the supplementary material. The observed global response indicates a decreasing trend of LAI response to drought while the model mean shows an increasing estimate.

The semi-desert biome dominates the LAI response as higher drought-vegetation correlations are observed (Figures 11G – I). Over the biome, there is more marked interannual variability which makes the biome an important player in global carbon cycling (Poulter *et al*., 2014). The response over the semi-desert in southern Africa is however weaker in comparison to the other semi-desert biomes.

The response over the Mediterranean vegetation in Australia is stronger than the Mediterranean vegetation over the rest of inland southern Africa. Over the biome, model simulates closer magnitudes in the latter than over Australia (Figures 11B and 9C).

Over the tropical forest biomes, there is a weaker response in Central Africa compared to Southern Africa and South America; the model simulates a closest response magnitude in South America (Figures 11D – F).
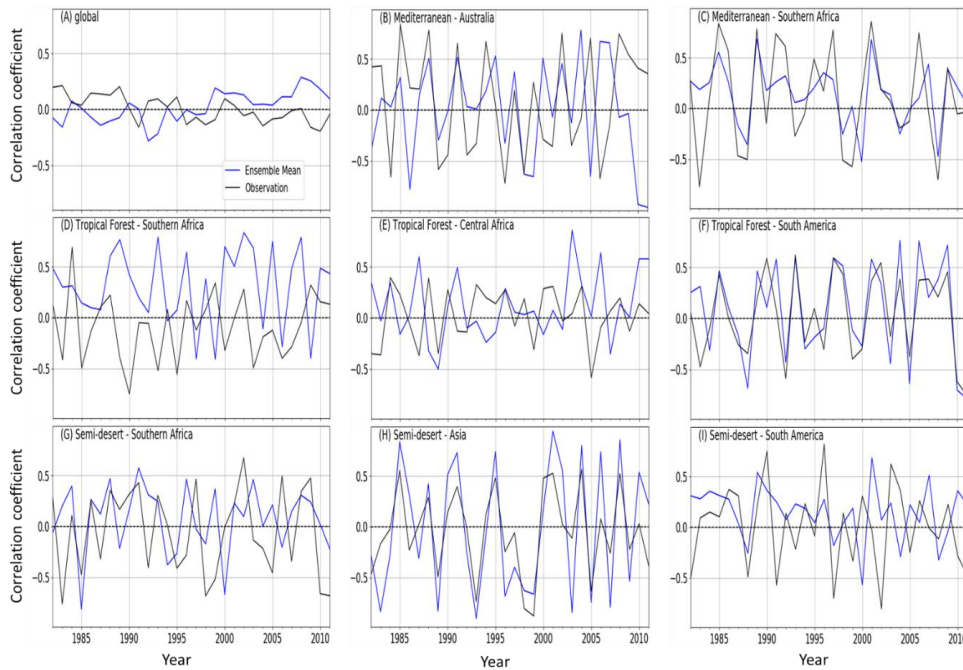
Figure 11. Correlations between SPEI (12-month timescale) and ensemble mean of LAI from TRENDY (blue line), GIMMS LAI (black line) for (A) Global (B) Mediterranean vegetation over Australia (C) Mediterranean vegetation over southern Africa (D) Tropical Forest over southern Africa (E) Tropical Forest over Central Africa (F) Tropical Forest over South America (G) Semi-desert biome over southern Africa (H) Semi-desert over Asia and (I) Semi-desert over South America.

4   Discussion

4.1   Relationship of LAI to phenological changes

LAI is a variable that is needed for global modelling of biogeochemistry, climate, ecology and hydrology and different primary production models (e.g., Running & Coughlan, 1988; Sellers *et al*., 1996; Bonan, 2002). In view of the need to run biogeochemical models at regional and global scales, accurate LAI data at moderate – high resolutions are crucial (Wang *et al*., 2004). The relationship between NDVI and LAI is applied as a support algorithm in MODIS LAI. Thus, from the viewpoint of availability of data, retrieving LAI from analyzing NDVI-LAI relationship remain the main perspective for high temporal resolution in regional and global-wide studies (Wang *et al*., 2004).

LAI showed a linear relationship with NDVI. This suggests that the NDVI is associated with the phenological changes of plants, the parts of surface cover class which contribute to the general

reflectance as well as the variations in the angle of solar zenith (Wang *et al*., 2004). Studies (e.g. Myoung *et al*., 2013) have however, found that the relationship between NDVI and LAI varies intra- and inter-annually; and both vegetation indices differ temporally and seasonally over deciduous forests, which are sometimes not accounted for in models that test their relationship (Wang *et al*., 2004). For instance, while the relationship is strong during periods of leaf production and senescence, no relationship is observed during the period of leaf constant due to NDVI saturation above certain LAI values (Xue and Su, 2017).

Although the present study found a strong linear relationship between the NDVI and LAI in southern Africa, other studies (Potithep *et al*., 2010; Towers *et al*., 2019) have shown the two indices are not always directly proportional. For example, both indices do not exhibit the same relationships over different eco-regions such as the Evergreen Broadleaf Forest, Deciduous Needleleaf Forest. Furthermore, other studies (Fan *et al*., 2008; Tian *et al*., 2017) found that the LAI may be better indicator of plant biomass and health because of the saturation associated with the NDVI, particularly in drylands. This makes the LAI more applicable in monitoring vegetation response to drought. Evaluating how the LAI differs from the NDVI over different biomes (such as dry savanna, tropical forest, etc), with regards to temporal difference is shown in Fig. S7. Both the LAI and NDVI show similar annual cycles over southern Africa, except for the Tropical forest and Mediterranean vegetation.

4.2 The importance of sub-monthly data in drought computation and monitoring

The data used to evaluate drought indices is CRUJRA. JRA is a reanalysis and has 6-hourly temporal resolution. Additionally, CRUJRA is the data used to force the DGVMs, so the drought indices are being calculated based on the same data the models use for their simulations. JRA is a reanalysis but the combined CRUJRA product uses the sub-monthly information from JRA, and is constrained to the monthly CRU observations. The comparisons of the data are shown in Figs. 5 and S6. It is useful to use data with shorter times because the study focuses on an evaluation of drought impact, which is sensitive to timescale. In drylands, for instance, the uncertainties associated with monthly data in drought monitoring are reduced when sub-monthly data are used (Mukherjee *et al*., 20117). With regards to the precipitation and temperature fields, the difference is negligible.

We note that, over different parts of the world, CRU has been widely validated against station data (Harris *et al*., 2020) and there is a high accuracy of the validation. Therefore, observed SPEI gives a high accuracy of measured drought. Another major advantage of using the observational-based CRU data is its spatial and temporal coverage. Station data are available for very few points and for limited times in the region of interest. The few data that are available are fraught with missing data, rendering them an unreliable data source (Harris *et al*., 2020).

4.3 Annual cycle of climate and vegetation in southern Africa

Climatologies of meteorological variables show that precipitation drops in JJA and SON seasons over the biomes except over Mediterranean vegetation. The dry condition that is experienced

during these seasons could be attributed to the subtropical high pressure system which suppresses rainfall by shifting the ITCZ (Inter-Tropical Convergence Zone) away from these regions (Naik and Abiodun, 2016).

Observations also show low LAI over some parts of southern Africa (please see Figure S2). The weak gradient in some parts of the region may be due to low winter rains produced by the frontal system which is not sufficient for growth of expanse vegetation (Lange *et al*., 1999). The aridification of the western part of southern Africa may be attributed to the influence of cold sea surface temperature (SSTs) of the Namibian Upwelling system along the Namibian coasts (Ward *et al*., 1983). The aridification does not only result in cessation of river discharge but also sediments that would have favored the growth of drier vegetation (Dupont, 2006).

For Fig. S5, some of the models do not capture this peak around September over the Mediterranean and Tropical biomes. One possible explanation is that the models do not well reproduce the changes in the biomass and leaf area cover around that period (due to phenological responses to environmental variables). For both biomes, spring rainfall contribute to vegetation growth in the region, which may not be well reproduced by the models. For Fig. 4, the magnitudes (< 0.5) of the observation-based LAI over (southern Africa) semi-desert biome is quite "high" because the region is a pseudo-desert, which experiences very high summer temperatures but does receives some rainfall, and the Okavango river is flowing through it permanently. This region is rich in biodiversity such as *Acacia spp* (trees) and *Aristida and Schmidita spp* (savanna) (see WWF 2001; Street and Prinsloo, 2013; Lawal *et al*., 2018.) Thus, a 0.5 LAI in the biome, which may be higher than other desert biomes, is reasonable in this region.

4.4   LAI response to drought in observation

Drought is becoming frequent and more intense in southern Africa (Masih *et al*., 2014). The frequent and stronger dry spells is observed in Fig. 6. Climate change is expected to increase the frequency and severity of droughts (Tables 2 and 3). The severity and longer durations of drought have enormous impacts on the already endangered vegetation biomes in the region (Hoffman *et al*., 2009). The results show that drought impacts on vegetation occur across the different seasons in the region. The seasonal difference in the response of vegetation to drought across biomes is influenced by numerous factors such as vegetation adaptive capacity and resilience, reproduction process and growth stage among others (Zeppel *et al*., 2014; Corlett, 2016). For instance, over the tropical forest biome, drought has the least impact on vegetation in the region, which could be because of the deeper rooting system of the vegetation which allows them access to soil at the deeper water table (El-Vilaly *et al*., 2017). It is reported that major drivers of vegetation resilience and productivity are precipitation and temperature which control the evapo-transpirative rate (Allen *et al*., 2010). It is worth noting that vegetation in southern Africa will be severely impacted if the trends continue in the same trajectory. For instance, the regions where there is a strong vegetation response to drought are experiencing wood encroachment and thus, will likely worsen based on the current trajectory of drought occurrence.

We note that the performance of drought indices is not only limited by the variables used in their computation but also by biomes and location where they are used (Xu *et al*., 2015). For example,

SPI which is calculated using simple methods and has adaptable timescales performs better than SPEI in arid regions (Begueria *et al.*, 2014). However, SPEI which requires more variables for its computation captures drought better in relatively humid zones (Begueria *et al.*, 2014). SPEI is however limited by the potential evapotranspiration (PET) because of its sensitivity to the variable (Xu *et al.*, 2015).

The vegetation situated at the borders of Botswana-Namibia and Mozambique-Zambia respond to droughts at an intermediate timescale (i.e. 9-month). The types of vegetation inhabiting these regions, which are well adapted to water shortage because of their physiological and morphological characteristics, takes prolonged period to respond to drought and thus, do not easily shows symptoms of water strain (Vicente-Serrano *et al.*, 2013). The activities through which vegetation minimize water loss include reduction in photosynthesis, reduced canopy cover (Schwinning & Sala, 2004). The capacity for vegetation to store water is one adaptation for low water ecosystems, as is reduced daytime stomatal conductance and CAM photosynthesis. The disparity in the timescales spatial distribution in models from obsevation might be because the parameters are represented and estimated in the models (Murray *et al.*, 2011). In addition, the models are not similar in their drought timescales simulations.

The varying response of the tropical forests in different regions may be because of the interplay of precipitation and temperature at different longitudes. Ahlstrom *et al* (2015) showed that temperature is particularly a strong factor in the response of this vegetation. Wang *et al* (2008) also reported that soil moisture variations play a key role in the magnitude of vegetation response. The weak response of LAI to drought over Madagascar and Angola may be attributed to the fact that the vegetation in these regions is able to store water for a long time which it uses during deficit (Chapotin *et al.*, 2006). It may also be because rainfall is not the main regulatory component in the growth of vegetation in these regions (Fuller and Prince, 1996). In regions such as Botswana and Namibia, vegetation is highly dependent on water availability for their ecosystem functions (Anyamba *et al.*, 2003). Please see Fig. S3 in the supplementary material for observed correlations at different timescales.

The seasonal response of LAI to drought varies and this could be attributed to many factors. For instance, the sensitivity of the semi-desert to water shortage makes them show quick response to drought (New, 2015). The response of vegetation to drought is particularly stronger in the MAM season, because it is during this period that fruit, leaves, and biomass are produced by vegetation (Zeppel *et al.*, 2014). Critical water requirements by vegetation for these developmental activities in the MAM season is the reason for the vegetation respond to droughts at a short timescale (Zeppel *et al.*, 2014). The strongest vegetation response (a correlation of about 0.92) is observed over the semi desert biome (which is in the semi-arid environment) in the JJA season. This is a region with vegetation which heavily depend on water for all their ecosystems functioning without which they would not survive (New, 2015). The drought response of tropical forest is weaker compared to all other biomes. Over the tropical forest biome, the fairly subtle drought response may be because the biome can be tolerant to drought, have stronger robust capacity and is therefore, not extremely impacted by droughts as are the other biomes (Gilgen *et al.*, 2005; Corlett, 2016).

The different response by the global biomes in different geographical locations may be because of climate variations and the sensitivity of LAI to climate variations (Ahlstrom *et al.*, 2015). The

dominance of LAI response to drought over the semi-desert biome could be attributed to the global bush encroachment and is in consonance with the increasing greenness (Donohue *et al*., 2009; Fensholt *et al.*, 2012; Andela *et al.*, 2013). Studies (Cai *et al*., 2014; Trenberth *et al*., 2014; Dai *et al*., 2013; Wang *et al*., 2014; Ahlstrom *et al*., 2015) have also found that increased and frequent ENSO events due to climate change have not only led to the expansion of LAI but could increase the water demand by semi-desert vegetation. This comparison is particularly important because until now, there has been little or no study on this.

4.5 How well the seasonal and interannual variations of LAI are captured in DGVM simulations

The models exhibit biases in the simulation of seasonal and interannual variations of LAI over southern Africa. Two major factors may be given for performance of the models. First, the influence of precipitation forcing data largely affect the seasonal cycle of LAI as well as the interannual variability (see Figs. 3 & S8). Although the difference between the forcing data for observed and modelled LAI (i.e. CRU and CRUJRA respectively) is small, it still influences the simulations by the DGVMs. The precipitation uncertainty has larger influence in some regions and biomes than others. For instance, the overestimation of LAI by models in arid biome of Namibia and Mediterranean vegetation of South Africa may be due to the irregularity in precipitation, whereby the precipitation changes are too little to be identified (in CRUJRA), as well as due the large spatial variability (Fekete *et al*., 2004; Greve *et al*., 2014). On the other hand, over the savanna biome of Angola, the underestimation is likely because of the sparse distribution of precipitation data, which permeates to CRUJRA (Fekete *et al*., 2004). Secondly, the differences in observed and simulated LAI may be due to the impacts of land use and land cover change on the latter (LULCC) on simulation, through soil moisture as well as evapotranspiration (Piao *et al*., 2015). LULCC exerts strong influence on water consumption, nutrient cycling, and root depth (Piao *et al*., 2007; Mango *et al*., 2011), and the extent of the influence also varies across biomes. For example, in MAM, over temperate grassland biome of South Africa, where the model underestimates LAI, the bias is likely because the models fail to simulate the frequency of evapotranspiration, which is about five times much less than the forest biome (Yang *et al*., 2015).

However, over most parts of the region, the correlation between observed and modelled LAI is strong, except in JJA season. This means that the models generally simulate the pattern of LAI distribution in southern Africa. We also note that, the lower correlations between observed and modelled LAI when the data were deseasonalized, is due to the sensitivity of LAI to variability and seasonality. These differences between observed and modelled system have impacts on how vegetation response to drought is captured, which we discuss in Section 4.6.

4.6 How well drought and LAI response is represented in DGVM simulations

The observed LAI is simulated within the models and calculated by GIMMS based on Mao and Yan, 2019. Lu *et al*., 2011 found that DGVMs perform better against observations than Earth system models (ESM) because they use observational-derived climate and can include more complex representations of vegetation processes. The ESM is a coupled model simulating its own climate, while the individual DGVMS models used in the present study are standalone, i.e. are

applied with observational based meteorological forcing, and thus we remove one uncertainty. Since offline studies target the DGVM itself, removing one possible issue (incorrect climate drivers), it became imperative to use DGVM to study drought impacts.

920   DGVMs simulate the vegetation characteristics and impacts of climate on them. The validation of DGVM simulations of variables such as LAI is quite difficult. This is because of the unavailability of data on large spatiotemporal scale for the different vegetation classes (Potter and Klooster, 1998). Studies (e.g. Potter and Klooster, 1998) have also shown that errors present in the prediction of plant functional types (PFTs) tend to spread to biomass prediction in the model, thus possibly
925   biasing estimates of carbon stored in terrestrial ecosystems. Nevertheless, the DGVMs used in this study simulate the spatial patterns of vegetation distribution though with a magnitude bias as shown in Fig. S2 in the supplementary material.

TRENDY models mostly simulate the temporal patterns of global and regional distributions of
930   LAI response to drought. The biases shown by the models have been attributed to the fact that the models do not factor land use changes (Ahlstrom *et al.,* 2015). This is evident in the simulation of LAI (please see Fig. S2).

The models' weaker simullations might also be because some of the DGVMs do not well reproduce the LAI magnitude. The negligible difference in the spatial distributions of SPEI of the
935   models could be due to fact that the model PET does not play a strong role in drought occurent in the southern Africa and that precipitation is the main driver of drought in the region. The variations in the characterization of hydrological processes in the models are also a source of uncertainty because they reinforce the bifurcation in runoff outputs which has cascading effects on biospheric changes and evapotranspiration (Murray *et al.*, 2011; Stewart *et al.*, 2004). Also see Fig. S4 for
940   correlations of the model ensemble median at different timescales. Another reason for the biases in the simulations may be to the design of the DGVM experimental set-up, which include the flux deviation between simulations without and with (Murray *et al.*, 2011).

4.7   Variations in observed and simulated vegetation response to drought, and implications on model development

945

The biases shown by models could be attributed to the different limitations of individual DGVMs, and addressing these shortcomings would improve models' performances. For example, the sub-optimal performance of CLM may be partly due to the inability of the model to capture foliage production and root system of vegetation for transpiration. The model is also unable to produce
950   savanna ecosystems, which it simulates by approximating vegetation of forest and grassland ecoregions (Dahlin *et al.*, 2020). In addition, the ineffective simulation of deciduousness would have contributed to the model biases in response simulations. Therefore, targeting these limitations is important for improving model's performance in simulating morphology and physiological functioning of vegetation biomes. Furthermore, the DGVMs (e.g. JULES, DLEM) used in the
955   study poorly replicate important ecological and physiological processes that are critical to capture the dynamics of savanna systems. Other DGVMs (e.g. JSBACH) poorly simulate significant environmental variables such as fire, which is very crucial for the vegetation growth cycle, particularly in the savanna biome (Thonicke *et al.*, 2001; Romps *et al.*, 2014; Kim *et al.*, 2018;

D'Onofrio *et al*., 2020). Also, over southern Africa, land use change (LUC) is a common and frequent occurrence, and is an important factor for vegetation turnover. However, most models do not well capture land management, which is an important driver of land cover change in the region. Thus, there is a need for future model development to account for rapid LUC over different regions. However, the disparity in observed and simulated response of vegetation to drought cannot be fully accounted by the DGVMs alone. The reanalysis (CRUJRA) has also shown some limitations in the simulation of climate variables. Compared to observation-based CRU, CRUJRA has closer magnitudes of maximum and minimum temperature, and addressing this would improve simulated response.

5   Summary and conclusions

Southern African vegetation is continually affected by drought. In this study, we estimated the spatiotemporal characteristics of meteorological drought in southern Africa using the Standardized Precipitation Evapotranspiration Index (SPEI) over a 30-year period (1982 – 2011). The severity of drought and its impacts on vegetation production were examined at various drought time-scales (1- to 24-month timescales) by correlating the drought index (SPEI) with GIMMS LAI at different timescales. We found that the LAI responds strongly (r = 0.6) to drought over the central and south eastern parts of the region, with weaker impacts (r < 0.4) over parts of Madagascar and Angola, mostly at a shorter time period (3-, 6-month timescale). We note that, comparing CRU to flux tower precipitation in Skukuza (Kwazulu Natal region) illustrates that CRU captures the timing of precipitation relatively well, though it underestimates the magnitude of dry season precipitation (Fig. S9). For seasonal responses, the semi-desert biome showed the strongest response (r = 0.95) to drought at 6-month timescale in the autumn season while the tropical forest biome shows the weakest response (r = 0.35) at 6-month timescale in the DJF season.

We assessed the relationship between the NDVI and LAI by computing a grid cell correlation of NDVI and LAI, and examined how well state-of-the-art dynamic global vegetation models (DGVMs) simulate LAI and its response to drought. The DGVM multi-model ensemble mostly overestimated the spatial and seasonal distribution of LAI response to drought in most parts of the region. The results also show that:

- The relationship between the NDVI and LAI is linear, implying that the vegetation index is connected to the changes in phenology of plant, reflectance and the angle of zenith variations from the surface cover class.

- The model ensemble simulates the correlation and timescale of LAI response to drought with biases.

- The model ensemble overestimates observed responses on the seasonal distribution of vegetation – drought correlations across different biomes.

- The spatial pattern of change of the LAI and SPEI are mostly similar during extreme dry and wet years, with the highest magnitudes of anomaly observed in the dry year of 1991. During this period, both variables also show an opposite and decreasing relationship, which is evident in their pattern correlation coefficient value of – 0.16.

The present study has shown how the LAI responds to drought across the different southern African biomes. Given the present spatial coverage of space monitoring of vegetation in the region, the methods used in the study may be extended towards monitoring and characterizing the impacts of droughts on land cover change, as this may permit real-time monitoring of extreme events on terrestrial vegetation (Yin *et al*., 2020; Moore *et al*., 2018). The findings of this study (e.g. timescales of LAI response to drought) could also be used for the development of drought early warning systems in agriculture and forestry sectors. This could assist in the mitigation of direct and indirect costs associated with vegetation production.

Furthermore, this study has applied eleven DGVMs to study how well DGVMs can reproduce the response of LAI in southern African vegetation to drought . While this study may have provided an insight into the capability of DGVMs to simulate vegetation response to drought, the results of the study can however, be improved in some ways. For example, we applied eleven models from the TRENDY DGVMs. For future studies, the number of models should be increased, perhaps from other model intercomparison experiments, because using more models, as well as better quantification, might capture uncertainty bettter in their simulation of drought response by vegetation. The limitation of the DGVMs can be addressed by optimizing the models so that their capability in reproducing vegetation indices is enhanced and better quantified. In addition, there is a need to improve mechanistic relationships in the models, which could be achieved by enhancing the model approximations which had been done to achieve computational efficiencies (Transtrum *et al*., 2016). Furthermore, simple phenomenological model could be developed from the complex model. These simple models would use correlations among observations, unlike mechanistic relationships which exploit causative individual constituent and suffer over-fitting problems (Transtrum *et al*., 2016). Lastly, there may be the need for hybridizing machine learning and mechanistic models (Fayyad *et al*., 1996; Mitchell, 1997) to simulate vegetation parameters. This is because machine learning models have shown certain advantage in the prediction of outcomes of complex mechanisms by using databases of inputs and outputs for a given task (Fayyad *et al*., 1996; Mitchell, 1997).

Data availability. Sources of data used in this work are provided in Section 2.1 and comprise CRU, CRUJRA, NDVI3g and Trendy DGVMs.

Author contributions. S.L. was responsible for conceptualization, developing the initial content of the manuscript, including literature search, data analysis and writing of the manuscript. S.S. and D.L. provided model outputs, and guided on data analysis. J.N., H.W.W., P.F, H.T. and B.H provided model output and guidance in terms of the article structure and finalization of the manuscript.

Competing interests. Authors declare no competing of interest.

Acknowledgements. The work was supported by the South African National Research Foundation (NRF).

References

Allen, C.D., Macalady, A.K., Chenchouni, H., Bachelet, D., McDowell, N.; Vennetier, M., and Gonzalez, P.: A global overview of drought and heat-induced tree mortality reveals emerging climate change risks for forests, For. Ecol. Manag., 259, 660–684, https://doi.org/10.1016/j.foreco.2009.09.001, 2010.

Ahlström, A., Raupach, MR., Schurgers, G., Smith, B., Arneth, A., Jung, M., Reichstein, M., Canadell, JG., Friedlingstein, P., Jain, AK., Kato, E., Poulter, B., Sitch, S., Stocker, BD., Viovy, N., Wang, YP., Wiltshire, A., Zaehle, S., andZeng, N.: The dominant role of semi-arid ecosystems in the trend and variability of the land CO2 sink, Science, 348, 895– 899, https://doi.org/10.1126/science.aaa1668, 2015.

Andela, N., Liu, YY., van Dijk, A. I. J. M., de Jeu, R. A. M., and McVicar, T. R.: Global changes in dryland vegetation dynamics (1988–2008) assessed by satellite remote sensing: Comparing a new passive microwave vegetation density record with reflective greenness data, Biogeosciences 10, 6657–6676, doi:10.5194/bg-10-6657-2013, 2013.

Anyamba, A., Justice, CO., Tucker, CJ., and Mahoney, R.: Seasonal to interannual variability of Vegetation and fires at SAFARI 2000 sites inferred from advanced very high resolution Radiometer time series data, Journal of Geophysical Research, vol 10 no D13, https://doi.org/10.1029/2002JD002464, 2003.

Beguería, S., Vicente-Serrano, SM., Reig, F., and Latorre, B.: Standardized precipitation evapotranspiration index (SPEI) revisited: parameter fitting, evapotranspiration models, tools, datasets and drought monitoring. International Journal of Climatology 34(10), 3001-3023, https://doi.org/10.1002/joc.3887, 2014.

Bonan, G. B., Oleson, KW., Vertenstein, M., Lewis, S., Zeng, X., Dai, Y., Dickinson, DE., and Yang, Z,: The land surface climatology of the NCAR land surface model coupled to the NCAR community climate model, Journal of Climate, 11, 1307 – 1327, https://doi.org/10.1175/1520-0442, 2002.

Chapotin, SM., Razanameharizaka, JH., and Holbrook, NM,: Water relations of baobab trees (Adansonia spp L.) during the rainy season. Does stem water buffer daily water deficit. Plant and Cell Environment 29, 1021-1032. doi. 10.1111-3040.2005.01456.x, 2006.

Cai, W., Borlace, S., Lengaigne, M., van Rensch, P., Collins, M., Vecchi, G., Timmermann, A., Santoso, A., McPhaden, MJ., Wu, M., England, L., H., Wang, G., Guilyardi, E., Jin, F.-F: Increasing frequency of extreme El Nino events due to greenhouse warming. Nat. Clim. Change 4, 111–116, doi:10.1038/nclimate2100, 2014.

Clark, D. B., Mercado, L. M., Sitch, S., Jones, C. D., Gedney, N., Best, M. J., Pryor, M., Rooney, G. G., Essery, R. L. H., Blyth, E., Boucher, O., Harding, R. J., Huntingford, C., and Cox, P. M.: The Joint UK Land Environment Simulator (JULES), model description – Part 2: Carbon fluxes and vegetation dynamics, Geosci. Model Dev., 4, 701–722, https://doi.org/10.5194/gmd-4- 701-2011, 2011.

Corlett, RT.: The Impacts of Droughts in Tropical Forests. Trends Plant Sci 21(7) 584-593, https://doi.org/10.1016/j.tplants.2016.02.003, 2016.

Dahlin, K. M., Fisher R.A., and Lawrence, P.J.: Environmental drivers of drought deciduous phenology in the Community Land Model, Biogeosciences, 12: 5061– 5074, https://doi.org/10.5194/bg-12-5061-2015, 2015.

Dahlin KM, Akanga D, Lombardozzi DL, Reed DE, Shirkey G, Lei C, Abraha M & J Chen.:

1090   Challenging a global land surface model in a local socio-environmental system. Land. 9(398): 1- 21. doi: 10.3390/land9100398, 2020

Dai, A.: Increasing drought under global warming in observations and models, Nat. Clim. Change **3**, 52–58, doi:10.1038/nclimate1633, 2013.

Department of Environmental Affairs (DEA). 2015. Climate Change Adaptation Plans for

1095   South African Biomes (ed. Kharika, J.R.M., Mkhize, N.C.S., Munyai, T., Khavhagali, V.P., Davis, C., Dziba, D., Scholes, R., van Garderen, E., von Maltitz, G., Le Maitre, D., Archibald, S., Lotter, D., van Deventer, H., Midgely, G. and Hoffman, T). Pretoria.

Donohue, R. J., McVicar, T. R., and Roderick, M. L.: Climate-related trends in Australian vegetation cover as inferred from satellite observations, 1981–2006. Glob. Change

1100   Biol. 15, 1025–1039, doi:10.1111/j.1365-2486.2008.01746.x, 2009.

D'Onofrio, D., Baudena, M., Lasslop, G., Nieradzik, L. P., Wårlind, D., and von Hardenberg, J.: Linking vegetation-climate-fire relationships in subsaharan africa to key ecological processes in two dynamic global vegetation models front. Environ. Sci. 8, 136. 10.3389/fenvs.2020.00136, 2020

1105 Driver A, Sink, KJ, Nel, JN, Holness, S, Van Niekerk, L, Daniels, F, Jonas, Z, Majiedt, PA, Harris, L and Maze, K 2012. National Biodiversity Assessment 2011: An assessment of South Africa's biodiversity and ecosystems. Synthesis Report. South African National Biodiversity Institute and Department of Environmental Affairs, Pretoria.

Dupont, LM.: Late Pliocene vegetation and Climate and Namibia (Southern Africa) derived

1110   From Palynology of ODP site 1082. Geochemistry, Geophysics and Geosystems, An AGU Journal. Vol 7 issue 5. doi: 10.1029.2005/gc001208, 2006.

Earth Summit, United Nation Conference on Environment and Development.: https://sustainabledevelopment.un.org/outcomedocuments/agenda21, 1992.

El-Vilaly, M.A.S., Didan, K., Marsh, S.E., van Leeuwen, W.J., Crimmins, M.A., and Munoz,

1115   A.B.: Vegetation productivity responses to drought on tribal lands in the four corners region of the Southwest USA, Front. Earth Sci., 12, 37–51, doi. https://doi.org/10.1007/s11707-017-0646-z, 2017.

Fan, L., Gao, Y., Brück, H., and Bernhofer, Ch.: Investigating the relationship between NDVI and LAI in semi-arid grassland in Inner Mongolia using in-situ measurements Theoretical

1120   and Applied Climatology, 10.1007/s00704-007-0369-2, 2008.

Fan, L. et al. Satellite observed pantropical carbon dynamics (2019). *Nat. Plants* **5**, 944–951

Fayyad, U., Piatetsky-Shapiro, G., Smyth, P. (Eds): From data mining to knowledge discovery Databases. AI Magazine 17, 37. 1996.

Fekete, B. M., C. J. Vörösmarty, J. O. Roads, and C. J. Willmott.: Uncertainties in

1125   precipitation and their impacts on runoff estimates, *J. Clim.*, **17**(2), 294– 304, doi: https://doi.org/10.1175/1520-0442(2004)017<0294:UIPATI>2.0.CO;2, 2004

Fensholt, R., Langanke, T., Rasmussen, K., Reenberg, A., Prince, S. D.,Tucker, C., Scholes, R. J., Le, Q. B., Bondeau, A., Eastman, R., Epstein, H., Gaughan, A. E., Hellden, U., Mbow, C., Olsson, L., Paruelo, J., Schweitzer, C., Seaquist, J., and

1130   Wessels. K.: Greenness in semi-arid areas across the globe 1981–2007—an Earth Observing Satellite based analysis of trends and drivers, Remote Sens. Environ. 121, 144–158. doi:10.1016/j.rse.2012.01.017, 2012.

FAO. 2000b (Eds). FAO/ESAF Handbook for Defining and Setting up a Food Security Information and Early Warning System (FSIEWS). Rome

1135 Forkel, Matthias, Nuno Carvalhais, Jan Verbesselt, Miguel D. Mahecha, Christopher S.R. Neigh,

and Markus Reichstein.: "Trend Change Detection in NDVI Time Series: Effects of Inter-Annual Variability and Methodology" *Remote Sensing* 5, no. 5: 2113-2144. https://doi.org/10.3390/rs5052113.: 2013.

Friederike E L Otto *et al* 2018 *Environ. Res. Lett.* 13 124010

1140   Fuller, DO., and Prince, SD.: Rainfall and foliar dynamics in tropical southern Africa: Potential impacts of global climatic change on savanna vegetation, *Clim Change 33,69-96.* 10.1007/BF00140514, 1996.

Gitelson, A. A.: Wide dynamic range vegetation index for remote quantification of biophysical characteristics of vegetation, Journal of Plant Physiology, vol. 161, no. 2, pp.
1145   165–173, https://doi.org/10.1078/0176-1617-01176, 2004.

Gielen B, De Boeck H, Lemmens CMHM, Valcke R, Nijs I, Ceulemans R.: Grassland species will not necessarily benefit from future elevated air temperatures: a chlorophyll fluorescence approach to study autumn physiology. *Physiol Plant 125:52–63,* https://doi.org/10.1111/j.1399-3054.2005.00539.x, 2005.

1150   Glantz, M.H., Betsill, M. and Crandall, K.: Food security in southern Africa. Assessing the use and value of ENSO information. National Center for Atmospheric Research, Boulder, CO, USA, 1997.

Goll, D. S., Vuichard, N., Maignan, F., Jornet-Puig, A., Sardans, J., Violette, A., Peng, S., Sun, Y., Kvakic, M., Guimberteau, M., Guenet, B., Zaehle, S., Penuelas, J., Janssens, I., and
1155   Ciais, P.: A representation of the phosphorus cycle for ORCHIDEE, Geosci. Model Dev., 10, 3745–3770, https://doi.org/10.5194/gmd-10-3745-2017, 2017.

Greve, P., B. Orlowsky, B. Mueller, J. Sheffield, M. Reichstein, and S. I. Seneviratne.: Global assessment of trends in wetting and drying over land, *Nat. Geosci.*, **7**(10), 716– 721, https://doi.org/10.1038/ngeo2247, 2014.

1160   Hao, Z., and AghaKouchak, A.: Multivariate standardized drought index: a parametric multi-index model, Advances in Water Resources, 57, 12– 18., https://doi.org/10.1016/j.advwatres.2013.03.009, 2013

Haverd, V., Smith, B., Nieradzik, L., Briggs, P. R., Woodgate, W., Trudinger, C. M., Canadell, J. G., and Cuntz, M.: A new version of the CABLE land surface model (Subversion
1165   revision r4601) incorporating land use and land cover change, woody vegetation demography, and a novel optimisation-based approach to plant coordination of photosynthesis, Geosci. Model Dev., 11, 2995– 3026, https://doi.org/10.5194/gmd-11-2995-2018, 2018.

Harris, I., Jones, PD., Osborn, TJ., and Lister, DH.: Updated high-resolution grids of monthly
1170   climatic observations – the CRU TS3.10 Dataset. Int. J. Climatol. 34(3), 623–642, doi: 10.1002/joc.3711, 2014.

Harris, I., Osborn, T. J., Jones, P., & Lister, D. Version 4 of the CRU TS monthly high-resolution gridded multivariate climate dataset. *Scientific Data***7**, 109 (2020)

Hoffman, MT., Carrick, PJ., and West, AG.: Drought, climate change and vegetation response
1175   in the succulent karoo, South Africa. South African Journal of Science S.Afr. j. sci. vol05:1-2*,* S. Afr. j. sci. vol.105 n.1-2 Pretoria Jan./Feb, 2009

Homdee, T., Pongput, K., and Kanae, S.: A comparative performance analysis of three standardized climatic drought indices in the Chi River basin, Thailand. Agriculture and Natural Resources, 50(3), 211– 219. https://doi.org/10.1016/j.anres.2016.02.002, 2016.
1180   Joetzjer E., Delire C., Douville H., Ciais P., Decharme B., D. Carrer, H. Verbeeck, M. De Weirdt,

D. Bonal.: Improving the ISBACC land surface model simulation of water and carbon fluxes and stocks over the Amazon forest, Geosci. Model Dev. 8, 1709-1727, doi:10.5194/gmd-8-1709-2015, 2015

Kato, E., Kinoshita, T., Ito, A., Kawamiya, M., and Yamagata, Y.: Evaluation of spatially explicit emission scenario of landuse change and biomass burning using a process-based biogeochemical model, Journal of Land Use Science, 8, 104–122, https://doi.org/10.1080/1747423X.2011.628705, 2013.

Kim, K.; Wang, M.C.; Ranjitkar, S.; Liu, S.H.; Xu, J.C.; Zomer, R.J. Using leaf area index (LAI) to assess vegetation response to drought in Yunnan province of China. *J. Mt. Sci.* 2017, *14*, 1863–1872.

Khosravi, H., Haydari, E., Shekoohizadegan, S., and Zareie, S.: Assessment the effect of drought on vegetation in desert area using landsat data Egypt. J. Remote Sens. Space Sci., 2007 (20), pp. S3-S12 ISSN 1110-9823, https://doi.org/10.1016/j.ejrs.2016.11.007, 2017.

Kim, J.B., Kerns, B.K., Drapek, R.J., Pitts, G.S., Halofsky J.E.: Simulating vegetation response to climate change in the Blue Mountains with MC2 dynamic global vegetation model, *Clim. Serv.*, 10 , pp. 20-32, https://doi.org/10.1016/j.cliser.2018.04.001, 2018.

Kwon, M., Kwon, H.H., Han, D.: Spatio-temporal drought patterns of multiple drought indices based on precipitation and soil moisture: a case study in South Korea Int. J. Climatol., 1–19 (2019), 10.1002/joc.6094, 2019.

Lange, C. B., Berger, W. H. , Lin, H.-L., Wefer, G. and Shipboard Scientific Party Leg 175.: The early Matuyama diatom maximum off SW Africa, Benguela current system (ODP Leg 175), *Mar. Geol.*, 161, 93–114, https://doi.org/10.1016/S0025-3227(99)00081-X, 1999

Lawal S.A. The response of southern African vegetation to drought in past and future climate. PhD Thesis University of Cape Town, South Africa (2018)

Lawal S., Lennard C., jack C. Wolski P., Hewitsin B., and Abiodun B.: The observed and model-simulated response of southern African vegetation to drought. https://doi.org/10.1016/j.agrformet.2019.107698, 2019.

Lawal S., Lennard C and Hewitson B.: Response of southern African vegetation to climate change at 1.5 and 2.0 degrees global warming above the pre-industrial level. Climate Services 16C 100134, 2019.

Le Quéré, C., Peters, G. P., Andres, R. J., Andrew, R. M., Boden, T. A., Ciais, P., Friedlingstein, P., Houghton, R. A., Marland, G., Moriarty, R., Sitch, S., Tans, P., Arneth, A., Arvanitis, A., Bakker, D. C. E., Bopp, L., Canadell, J. G., Chini, L. P., Doney, S. C., Harper, A., Harris, I., House, J. I., Jain, A. K., Jones, S. D., Kato, E., Keeling, R. F., Klein Goldewijk, K., Körtzinger, A., Koven, C., Lefèvre, N., Maignan, F., Omar, A., Ono, T., Park, G.-H., Pfeil, B., Poulter, B., Raupach, M. R., Regnier, P., Rödenbeck, C., Saito, S., Schwinger, J., Segschneider, J., Stocker, B. D., Takahashi, T., Tilbrook, B., van Heuven, S., Viovy, N., Wanninkhof, R., Wiltshire, A., and Zaehle, S.: Global carbon budget 2013, Earth Syst. Sci. Data, 6, 235–263, https://doi.org/10.5194/essd-6-235-2014, 2014.

Lienert, S., and Joos, F.: A Bayesian ensemble data assimilation to constrain model parameters and land-use carbon emissions, Biogeosciences, 15, 2909–2930, https://doi.org/10.5194/bg-15- 2909-2018, 2018.

Lu, E., Luo, Y., Zhang, R., Wu, Q., and Liu, L.: Regional atmospheric anomalies responsible

for the 2009–2010 severe drought in China, J. Geophys. Res., 116 (D21), https://doi.org/10.1029/2011JD015706, 2011.

Lu, E., Cai, W., Jiang, Z., Zhang, Q., Zhang, C., Higgins, R.W., and Halpert, M.S.: The day-to-day monitoring of the 2011 severe drought in China, Clim. Dynam, https://doi.org/10.1007/s00382-013-1987-2, 2014.

Luo, L.; Tang, W.; Lin, Z.; Wood, E.F. Evaluation of summer temperature and precipitation predictions from NCEP CFSV2 retrospective forecast over China. *Clim. Dyn.*, *41*, 2213–2230, https://doi.org/10.1007/s00382-013-1927-1, 2013.

Mango, L. M., A. M. Melesse, M. E. McClain, D. Gann, and S. G. Setegn (2011), Land use and climate change impacts on the hydrology of the upper Mara River Basin, Kenya: Results of a modeling study to support better resource management, *Hydrol. Earth Syst. Sci.*, **15**(7), 2245– 2258.

Mao, J., and Yan, B.: Global Monthly Mean Leaf Area Index Climatology, 1981-2015. ORNL DAAC, Oak Ridge, Tennessee, USA. https://doi.org/10.3334/ORNLDAAC/1653, 2019.

Masih, I., Uhlenbrook, S., Maskey, S., and Smakhtin, V.: Stream-flow trends and climate linkages in the Zagros Mountain, Iran. Clim. Change, 104, 317–338, doi:10.1007/s10584-009-9793-x, 201, 2014.

Mauritsen, T., Bader, J., Becker, T., Behrens, J., Bittner, M., Brokopf, R., Brovkin, V., Claussen, M., Crueger, T., Esch, M., Fast, I., Fiedler, S., Popke, D., Gayler, V., Giorgetta, M., Goll, D., Haak, H., Hagemann, S., Hedemann, C., Hohenegger, C., Ilyina, T., Jahns, T., Jimenez Cuesta de la Otero, D., Jungclaus, J., Kleinen, T., Kloster, S., Kracher, D., Kinne, S., Kleberg, D., Lasslop, G., Kornblueh, L., Marotzke, J., Matei, D., Meraner, K., Mikolajewicz, U., Modali, K., Möbis, B., Müller, W., Nabel, J. E. M. S., Nam, C., Notz, D., Nyawira, S., Paulsen, H., Peters, K., Pincus, R., Pohlmann, H., Pongratz, J., Popp, M., Raddatz, T., Rast, S., Redler, R., Reick, C., Rohrschneider, T., Schemann, V., Schmidt, H., Schnur, R., Schulzweida, U., Six, K., Stein, L., Stemmler, I., Stevens, B., von Storch, J., Tian, F., Voigt, A., de Vrese, P., Wieners, K.-H., Wilkenskjeld, S., Roeckner, E., and Winkler, A Developments in the MPI-M Earth System Model version 1.2 (MPI-ESM1.2) and its response to increasing CO2, J. Adv. Model. Earth Sy., https://doi.org/10.1029/2018MS001400, 2018.

McKee, T. B., Doesken, N. J. and Kleist, J.: The relationship of drought frequency and duration to time scales. Proc. Eight Conf. on Applied Climatology. Anaheim, CA, Amer. Meteor. Soc. 179–184, 1993

Melillo, J.: Climate change, risky business, and a call to action for ecologists. Ecosystem Health and Sustainability 1(1), https://doi.org/10.1890/EHS14-0016.1, 2015.

Melton, J. R., and Arora, V. K.: Competition between plant functional types in the Canadian Terrestrial Ecosystem Model (CTEM) v. 2.0, Geosci. Model Dev., 9, 323–361, https://doi.org/10.5194/gmd-9-323-2016, 2016.

Mitchell TM. 1997*Machine learning*. Boston, MA: McGraw-Hill Series in Computer Science.

Mitchell, TD., and Jones, PD.: An improved method of constructing a database of monthly climate observations and associated high- resolution grids. Int. J. Climatol. 25: 693–712, https://doi.org/10.1002/joc.1181, 2005.

Moore, B., Crowell, S. M. R., Rayner, P. J., Kumer, J., O'Dell, C. W., O'Brien, D., Utembe, S., Polonsky, I., Schimel, D., and Lemen, J.: The potential of the geostationary carbon cycle observatory (GeoCarb) to provide multi-scale constraints on the carbon cycle in the

Americas. Frontiers in Environmental Science, **6**, 109,
https://doi.org/10.3389/fenvs.2018.00109 , 2018.

Mukherjee, N., Zabala, A., Huge, J., Nyumba, T. O., Esmail, B. A., and Sutherland, W.
1275   J.: Comparison of techniques for eliciting views and judgements in decision-
making. Methods in Ecology and Evolution, **9**, 54– 63, https://doi.org/10.1111/2041-
210X.12940, 2017.

Müller C, Cramer W, Hare WL, Lotze-Campen H.: Climate change risks for African
agriculture. Proc Natl Acad Sci USA 108(11):4313–4315. doi:10.1073/pnas.1015078108,
1280   2011.

Murray, SJ., Foster, PN., and Prentice, IC.: Evaluation of global continental hydrology as
simulated by the Land-surface Processes and eXchanges Dynamic Global Vegetation
Model. Hydrology and Earth System Sciences 15: 91–105, https://doi.org/10.5194/hess-
15-91-2011, 2011.

1285 Myoung, B., Choi, Y.-S., Hong, S., and Park S. K.: Inter- and intra-annual variability of
vegetation in the northern hemisphere and its association with precursory meteorological
factors, *Global Biogeochem. Cycles*, 27, 31– 42, doi:10.1002/gbc.20017, 2013.

Naik, M., and Abiodun, BJ.: Potential impacts of forestation on future climate change in
Southern Africa. International Journal of Climatology. doi:10.1002/joc.4652, 2016.

1290 Naumann, G., Alfieri, L., Wyser, K., Mentaschi, L., Betts, R.A., Carrao, H., Spinoni, J., Vogt, J.,
Feyen, L.: Global changes in drought conditions under different levels of
warming. Geophys. Res. Lett., *45*, 3285–3296., https://doi.org/10.1002/2017GL076521,
2018.

New, M. G., M. Hulme, and P. D. Jones.: Representing twentieth-century space–time
1295   climate variability. Part II: Development of 1901–1996 monthly terrestrial climate
fields. *J. Climate,* pg. 2217- 2238, , doi: https://doi.org/10.1175/1520-
0442(2000)013<2217:RTCSTC>2.0.CO;2, 1999.

New M, Hulme M, Jones PD. 2000. Representing twentieth century space-time climate
variability. II: development of 1901–1996 monthly grids of terrestrial surface
1300   climate. *Journal of Climate* **13**: 2217– 2238, , doi: https://doi.org/10.1175/1520-
0442(2000)013<2217:RTCSTC>2.0.CO;2, 2000.

New, M.: Are semi-arid regions climate change hot-spots? Evidence from Southern Africa,
African Climate and Development Initiative (ACDI) blog, 2015.

Oleson, K. W., Dai, Y., Bonan, G., Bosilovich, M., Dickinson, R., Dirmeyer, P., Hoffman, F.,
1305   Houser, P., Levis, S., Niu, G.-Y., Thornton, P., Vertenstein, M., Yang, Z.-L. and Zeng,
X.: Technical description of the Community Land Model (CLM). NCAR Tech. Note
NCAR/TN-461+STR, 174 pp, 2004.

Oleson, K., Lawrence, D., Bonan, G., Drewniak, B., Huang, M., Koven, C., Levis, S., Li, F.,
Riley, W., Subin, Z., Swenson, S., Thornton, P., Bozbiyik, A., Fisher, R., Heald, C.,
1310   Kluzek, E., Lamarque, J., Lawrence, P., Leung, L., Lipscomb, W., Muszala, S., Ricciuto,
D., Sacks, W., Tang, J., and Yang, Z.: Technical Description of version 4.5 of the
Community   Land   Model   (CLM),   NCAR,   available   at:
http://www.cesm.ucar.edu/models/cesm1.2/ clm/CLM45_Tech_Note.pdf, 2013.

Palmer WC.: Keeping track of crop moisture conditions, nationwide: the new Crop Moisture
1315   Index. Weatherwise 21:156–161, https://doi.org/10.1080/00431672.1968.9932814, 1965.

Piao, S., P. Friedlingstein, P. Ciais, N. de Noblet-Ducoudre, D. Labat, and S.

Zaehle.: Changes in climate and land use have a larger direct impact than rising CO_2 on global river runoff trends, *Proc. Natl. Acad. Sci. U.S.A.*, **104**(39), 15,242– 15,247, doi:10.1073/pnas.0707213104, 2007

1320 Pinzon, J. E. and Tucker, C. J.: A Non-Stationary 1981-2012 AVHRR NDVI3g Time Series, Remote Sensing, 6, 6929–6960, https://doi.org/10.3390/rs6086929, 2014.

Potithep, S., Nasahara, N., Muraoka, H., Nagai, S. and Suzuki, R.: What is the actual relationship between LAI and VI in a deciduous broadleaf forest. International Archives of the Photogrammetry, Remote Sensing and Spatial Information Science 38, 609–614, 2010.

1325 Poulter, B., Frank, D., Ciais, P., Myneni, R. B., Andela, N., Broquet, G. J. B, Canadell, J. G., Chevallier, F., Liu, Y. Y., Running, S. W., Sitch, S., and van der Werf, G. R.: Contribution of semi-arid ecosystems to interannual variability of the global carbon cycle. Nature 509, 600–603, doi:10.1038/nature13376pmid:2484788, 2014.

Potter, C.S., and Klooster, S.A.: Global model estimates of carbon and nitrogen storage in
1330 litter and soil pools: response to change in vegetation quality and biomass allocation. Tellus, 49B, 1, https://doi.org/10.3402/tellusb.v49i1.15947, 1997.

Potter, CS, and Klooster, SA.: Dynamic global vegetation modelling for prediction of plant types and biogenic trace gas fluxes. Global Ecol Biogeogr 8:473–488, https://doi.org/10.1046/j.1365-2699.1999.00152.x, 1998.

1335 Rahimzadeh-Bajgiran, P., Omasa, K., & Shimizu, Y.: Comparative evaluation of the Vegetation Dryness Index (VDI), the Temperature Vegetation Dryness Index (TVDI) and the improved TVDI (iTVDI) for water stress detection in semi-arid regions of Iran. *ISPRS Journal of Photogrammetry and Remote Sensing, 68*, 1–12. doi:10.1016/j.isprsjprs.2011.10.009, 2012.

1340 Rezaei M, Sameni A, Shamsi SRF, Bartholomeus H.: Remote sensing of land use/cover changes and its effect on wind erosion potential in southern Iran. Peerj. doi:10.7717/peerj.1948, 2016.

Reuter, M., Bösch, H., Bovensmann, H., Bril, A., Buchwitz, M., Butz, A., Burrows, J. P., O'Dell, C. W., Guerlet, S., Hasekamp, O., Heymann, J., Kikuchi, N., Oshchepkov, S., Parker, R.,
1345 Pfeifer, S., Schneising, O., Yokota, T., and Yoshida, Y.: A joint effort to deliver satellite retrieved atmospheric CO2 concentrations for surface flux inversions: the ensemble median algorithm EMMA, Atmos. Chem. Phys., 13, 1771–1780, doi:10.5194/acp-13-1771- 2013, 2013.

Romps, D.M., Seeley, J.T., Vollaro, D., Molinari J. (2014). Projected increase in lightning
1350 strikes in the United States due to global warming Science, 346 (6211) , pp. 851-854.

Running, S. W., & Coughlan, J. C.: A general model of forest ecosystem processes for regional applications. Ecological Modelling, 42, 124 – 154., https://doi.org/10.1016/0304-3800(88)90112-3, 1988.

Santin-Janin, H., Garel, M., Chapuis, J.-L., and Pontier, D.: Assessing the performance of
1355 NDVI as a proxy for plant biomass using non-linear models: a case study on the Kerguelen archipelago Polar Biology, 32 (2009), pp. 861-871, https://doi.org/10.1007/s00300-009-0586-5, 2009.

Schaefer, K., Schwalm, C. R., Williams, C., Altaf Arain, M., Barr, A., Chen, J. M., et al.: A model-data comparison of gross primary productivity: Results from the North
1360 American Carbon Program site synthesis. Journal of Geophysical Research, 117, G03010. http://dx.doi.org/10.1029/2012JG001960, 2012.

Schwinning, S., Starr, B. I., and Ehleringer, J. R., Summer and winter drought in a cold

desert ecosystem (Colorado Plateau) part II: effects on plant carbon assimilation and growth. Journal of Arid Environments 61:61–78., https://doi.org/10.1016/j.jaridenv.2004.07.013, 2005.

Sinclair, REA., and Beyers, RL.: African Biomes. Ecology. doi.10.10/OBO978199830060., 2015.

Singh, S.K., A. Chamorro, M.S. Srinivasan and L. Breuer.: A copula-based analysis of severity-duration-frequency of droughts in six climatic regions of New Zealand. Journal of Hydrology (New Zealand), 56(1):13, https://search.informit.org/doi/10.3316/informit.665171198981944, 2017.

Sellers, P. J., Randall, D. A., Collatz, G. J., Berry, J. A., Field, C. B., Dazlich, D. A., Zhang, C., and Collelo, GD., and Bounuoa, L.: A revised land surface parameterization (SIB2) for Atmospheric GCMs: Part I. Model formulation. Journal of Climate, 9, 676 – 705., https://doi.org/10.1175/1520-0442, 1996.

Sitch, S., Huntingford, C., Gedney, N., Levy, P.E., Lomas, M., Piao, S.L., Betts, R.,Ciais, P., Cox, P., Friedlingstein, P., Jones, CD., Prentice, IC., and Woodward, FI.*:* Evaluation of the terrestrial carbon cycle, future plant geography and climate-carbon cycle feedbacks using five Dynamic Global Vegetation Models (DGVMs). *Global Change Biol.*, 14, 2015– 2039, https://doi.org/10.1111/j.1365-2486.2008.01626.x, .2008.

Stagge, J. H., Tallaksen, L.M., Gudmundsson, L., van Looon, A.F. and Stahl, K.: Pan-European comparison of candidate distributions for climatological drought indices (SPI and SPEI) Hydrology in a Changing World: Environmental and Human Dimensions Proceedings of FRIEND -Water 2014, Montpellier, France, October 2014 (IAHS Publ. 363, 2014.

Stewart, IT., Cayan, DR., Dettinger, MD.: Changes in snowmelt runoff timing in western North America under a 'business as usual' climate change scenario. Climatic Change 62(1–3): 217–232., https://doi.org/10.1023/B:CLIM.0000013702.22656.e8, 2004.

Street RA & Prinsloo G. (2013). Commercially Important Medicinal Plants of South Africa: A Review. *Journal of Chemistry Vol 2013. Article ID 205048 16pages.*

Sultan, B., and Gaetani, M.: Agriculture in West Africa in the twenty-first century: Climate change and impacts scenarios, and potential for adaptation. Frontiers in Plant Science, **7**, 1– 20, doi: 10.3389/fpls.2016.01262, 2016.

Thenkabail, P.S., Gamage, M.S.D.N., Smakhtin, V.U., 2004. The use of remote sensing data for drought assessment and monitoring in Southwest Asia. Research report. 85, Int. Water. Manage. Inst. Colombo, Sri Lanka

Teuling, AJ., vanLoon A., Seneviratne S., Lehner, M., Aubinet M., Heinesch B., Bernhofer, C., Grunwald, T., Prasse, H., and Spank, U.: Spank Evapotranspiration amplifies European summer drought Geophys. Res. Lett., 40 (10), pp. 2071-2075, https://doi.org/10.1002/grl.50495, 2013.

Tian, H. Q., Chen, G. S., Lu, C. Q., Xu, X. F., Hayes, D. J., Ren, W., Pan, S. F., Huntzinger, D. N., and Wofsy, S. C.: North American terrestrial CO2 uptake largely offset by CH4 and N2O emissions: toward a full accounting of the greenhouse gas budget, Climatic Change, 129, 413–426, https://doi.org/10.1007/s10584- 014-1072-9, 2015.

Tian, F., Brandt, M., Liu, Y. Y., Rasmussen, K., and Fensholt, R.: Mapping gains and losses in woody vegetation across global tropical drylands. *Global Change Biology*, 23(4), 1748– 1760. https://doi.org/10.1111/gcb.13464, 2017.

Towers, Pedro C.; Strever, Albert; Poblete-Echeverría, Carlos.: "Comparison of Vegetation

Indices for Leaf Area Index Estimation in Vertical Shoot Positioned Vine Canopies with
1410 and without Grenbiule Hail-Protection Netting" *Remote Sens.* 11, no. 9: 1073.
https://doi.org/10.3390/rs11091073, 2019.

Transtrum, MK., Qiu, P.: Bridging mechanistic and phenomenological models of complex
biological systems. PLoS Comput Biol 12(5):e1004, 915,
https://doi.org/10.1371/journal.pcbi.1004915, 2016.

1415 Trenberth, K. E., A. Dai, G. van der Schrier, P. D. Jones, J. Barichivich, K. R. Briffa, and J.
Sheffield.: Global warming and changes in drought, *Nat. Clim.
Change*, **4**(1), 17– 22., https://doi.org/10.1038/nclimate2067, 2014.

Thonicke, K., Venevsky, S., Sitch, S., and Cramer, W.: The role of fire disturbance for global
vegetation dynamics: coupling fire into a Dynamic Global Vegetation Model, Global Ecol.
1420 Biogeogr., 10, 661–677, 2001.

Ujeneza, E., and Abiodun, BJ., Drought regimes in Southern Africa and how well GCMs
simulate them? Clim Dyn, 44 (5), 1595-1609, 10.1007/s00382-014-2325-z, 2014.

Ujeneza E.L.Simulating the Characteristics of Droughts in Southern Africa M.Sc. Thesis
University of Cape Town, South Africa (2014)

1425 United Nations Environmental Protection – UNEP (2008). Atlas of changing environment.
Biomes of Africa. *Nairobi, Kenya: UNEP*.

Vicente-Serrano, S.M. and López-Moreno, J.I.: The influence of atmospheric circulation
at different spatial scales on winter drought variability through a semi-arid climatic
gradient in northeast Spain. *International Journal of Climatology*, **26**(11), 1427– 1453,
1430 https://doi.org/10.1002/joc.1387, 2006.

Vicente-Serrano, SM., Beguería, S., López-Moreno, JI., Angulo, M. El Kenawy, A.: A new
global 0.5° gridded dataset (1901-2006) of a multiscalar drought index: comparison with
current drought index datasets based on the Palmer Drought Severity Index. Journal of
Hydrometeorology 11: 1033–1043, https://doi.org/10.1175/2010JHM1224.1, 2010.

1435 Vicente-Serrano, S. M, Bengueria, S., and Lopez-Moreno, J.:Comment on ''Characteristics and
trends in various forms of the Palmer Drought Severity Index (PDSI) during 1900–2008''
by Aiguo Dai.J. Geophys. Res.,116,D19112, doi:10.1029/2011JD016410, 2011.

Vicente-Serrnao, SM., Gouvelia, C., Camarero, J.J, Begueria, S., Trigo, R., Lopez-Moreno, JI.,
Azorin-Molina, A., Pasho, E., Lorenzo-Lacruz., J, Revuelto, J., Moran-Tejeda, E., and
1440 Sanchez-Lorezo, A.: Response of vegetation to drought time-scales across global land
biomes. *PNAS Vol 110 1. www.pnas.org/cgi/doi/10.1073/pnas.1207068110,* 2012.

Vicente-Serrano, S.M. (2013) Spatial and temporal evolution of precipitation droughts in Spain
in the last century. In: C.C.-L. Martínez and F.V. Rodríguez (Eds.) *Adverse Weather in
Spain*, pp. 283– 296. Madrid, Spain: Consorcio de Compensación de Seguros.

1445 Vicente-Serrano, Sergio M. and National Center for Atmospheric Research Staff (Eds).:
"The Climate Data Guide: Standardized Precipitation Evapotranspiration Index (SPEI)."
Retrieved from https://climatedataguide.ucar.edu/climate-data/standardized-precipitation-
evapotranspiration-index-spei., 2015.

Wang, Q., Tenhunen, J., Dinh, NQ., Reichstein, M., Vesala, T., and Keronen, P.: Similarities in
1450 ground- and satellite-based ndvi time series and their relationship to physiological
activity of a Scots pine forest in Finland. Remote Sensing of Environment 93**,** 225–237.,
10.1016/j.rse.2004.07.006, 2004.

Wang A, Li, KY., and Lettenmailer DP.: Integration of the Variable Infiltration Capacity

Model Soil hydrology scheme into the Community Land Model. Climate and Dynamics, https://doi.org/10.1029/2007JD009246, 2008.

Wang S 2010 Three characteristics of meteorological drought in southwest china *China Meteorol. News* **3** 3–4 (in Chinese)

Wang, X., Piao, S., Ciais, P., Friedlingstein, P., Myneni, R.B., Cox, P., Heimann, M., Miller, J., Peng, S., Wang, T., Yang, H., and Chen, A.: A two-fold increase of carbon cycle sensitivity to tropical temperature variations. Nature **506**, 212–215 (2014). doi:10.1038/nature12915 pmid:24463514, 2014.

Ward, J. D., Seely, M. K., and Lancaster, N.: On the antiquity of the Namib, *S. Afr. J. Sci.*, 79, 175–183, 1983.

Wilhite, D.A., and Glantz, M.H.: Understanding the drought phenomenon: the role of definitions, Water Int., 10 (3), pp. 111-120, https://doi.org/10.1080/02508068508686328, 1985.

Woodward, FI., and Lomas, MR.: Vegetation-dynamics – simulating responses to climate Change. Biological Reviews 79, 643 – 670, https://doi.org/10.1017/S1464793103006419, 2004.

Wolski P, Otto F E L, Odoulami R and New M 2018 Attribution of the three-year drought that triggered the 2017 'Day Zero' water crisis in Cape Town, South Africa. In explaining extreme events of 2017 from a climate perspective *Spec. Suppl. Bull. Am. Meteorol. Soc.*

Wolski P 2018 How severe is Cape Town's 'Day Zero' drought? *Significance* 15 24–7

WRI (World Resources Institute). 2000. World resources 2000–2001. People and ecosystems:

WWF(2001). Assessed on May 17, 2017.
http://www.wwf.org.za/our_work/initiatives/grasslands.cfm

Xu, K., Yang, D., Yang, H., Li, Z., Qin, Y., Shen, Y.: Spatio-temporal variation of drought in China during 1961–2012: a climatic perspective J. Hydrol., 526, pp. 253-264, 10.1016/j.jhydrol.2014.09.047, 2015.

Xue, J., and Su, B.: Significant remote sensing vegetation indices: a review of developments and applications, J. Sens., p. 17, https://doi.org/10.1155/2017/1353691, 2017.

Yang, Y, J., Fang, J, W, Ma and Wang, W.: Relationship between variability in aboveground Net primary production in global grasslands. Geophy Res Lett Vol 35, l23710, doi:10.1029/2008GLO35408, 2008.

Yang, H., Piao, S., Zeng, Z., Ciais, P., Yin, Y., Friedlingstein, P., Sitch, S., Ahlström, A., Guimberteau, M., Huntingford, C., Levis, S., Levy, P. E., Huang, M., Li, Y., Li, X., Lomas, M. R., Peylin, P., Poulter, B., Viovy, N., Zaehle, S., Zeng, N., Zhao, F., & Wang, L. (2015). Multicriteria evaluation of discharge simulation in Dynamic Global Vegetation Models. *Journal of Geophysical Research: Atmospheres*, **120**, 7488– 7505. https://doi.org/10.1002/2015JD023129

Yin, Y., Byrne, B., Liu, J., Wennberg, P., Davis, K. J., Magney, T., et al.: Cropland carbon uptake delayed and reduced by 2019 Midwest floods. AGU Advances, 1, e2019AV000140. https:// doi.org/10.1029/2019AV000140., 2020.

Zaehle, S., Ciais, P., Friend, A. D., and Prieur, V.: Carbon benefits of anthropogenic reactive nitrogen offset by nitrous oxide emissions, Na. Geosci., 4, 601–605, https://doi.org/10.1038/NGEO1207, 2011.

Zeppel MJB, Wilk JV and Lewis JD.: Impacts of extreme precipitation on plants. *Biogeosciences, 11, 3083 – 3093. doi. 10.5194/bg-11 3083-2004,* 2014.

Zhang, L., Xiao, J., Li, J., Wang, K., Lei, L., and Guo, H.: The 2010 spring drought reduced

1500   primary productivity in southwestern China, Environ. Res. Lett., 7 (4), p. 045706, 10.1088/1748-9326/7/4/045706, 2012.

Zhao, C., Deng, X., Yuan, Y., Yan, H., and Liang, H.: Prediction of drought risk based on the WRF model in yunnan province of China Adv. Meteorol., pp. 1-9, https://doi.org/10.1155/2013/295856, 2013.

1505   Zhu, X., Liu, D., 2015. Improving forest aboveground biomass estimation using seasonal Landsat NDVI time-series. ISPRS J. Photogr. Rem. Sens. 102, 222–231.